

Solar neutrino results from Super-Kamiokande

Satoru Yamada

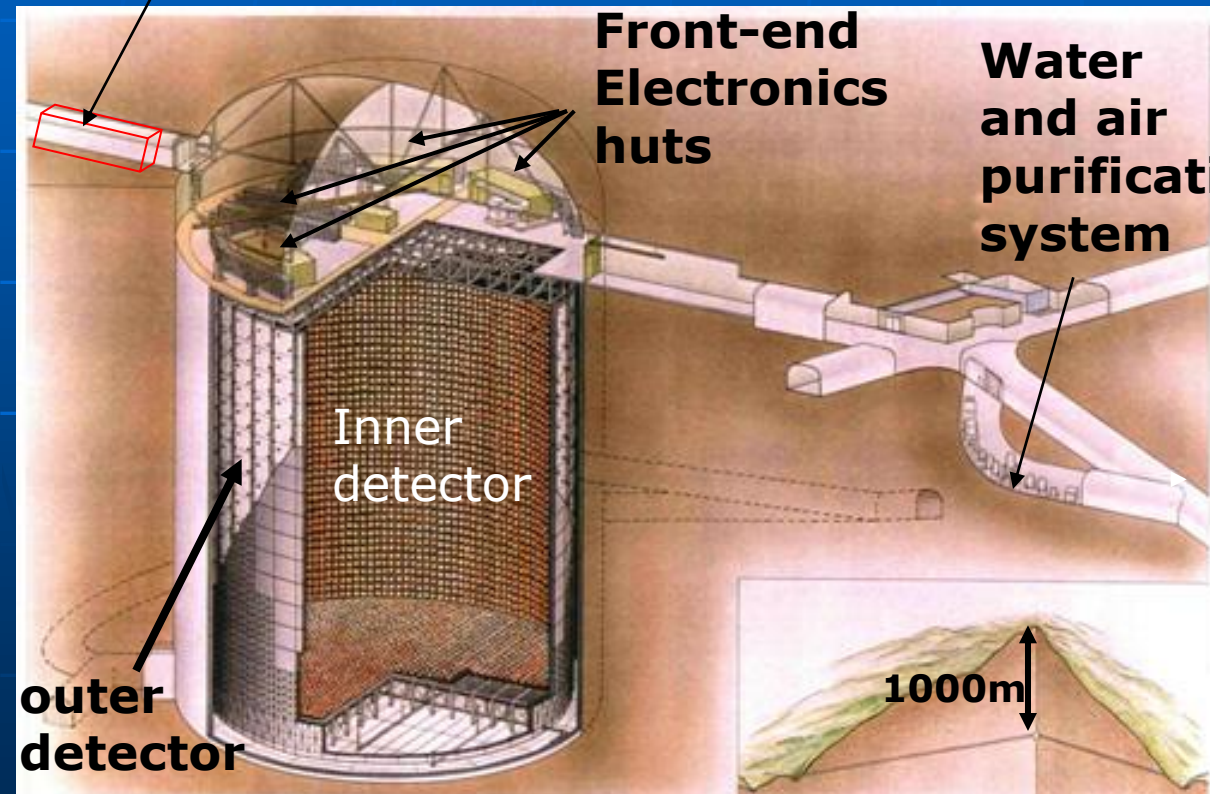
for the Super-Kamiokande collaboration
Institute of cosmic ray research, University of Tokyo

1, SK solar neutrino measurement

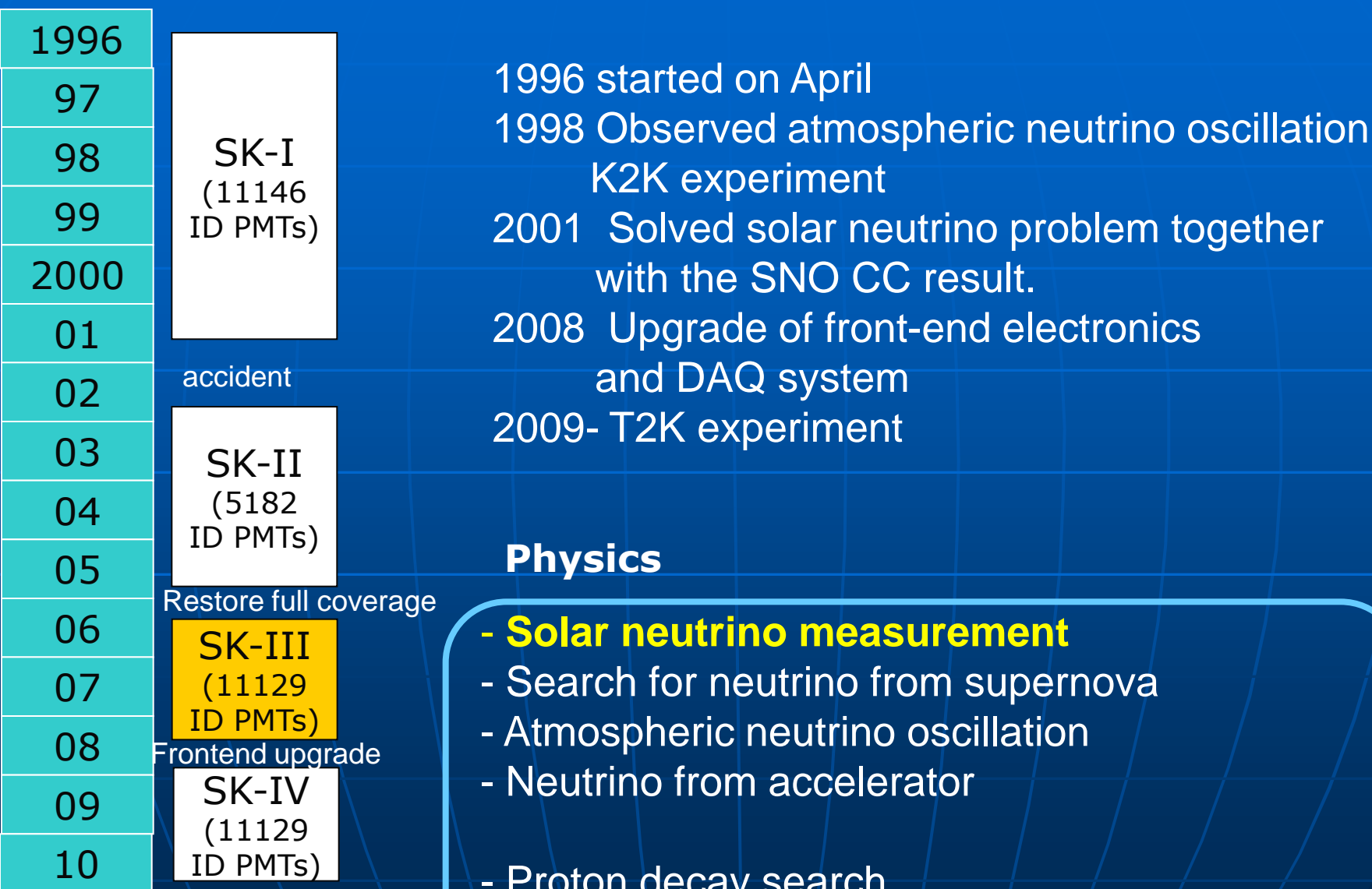
Super Kamiokande detector

electron
linear
accelerator
for energy
calib.

- 50 kton water Cherenkov detector at 1000m underground (2700 w.e.)
- 32kton inner detector: 11129 PMTs (20inch)
- Fiducial volume : 22.5kton (2m from the wall)
- Outer detector : 1885 PMTs (8inch) for cosmic ray muon veto



Super Kamiokande experiment



Physics

- **Solar neutrino measurement**
- Search for neutrino from supernova
- Atmospheric neutrino oscillation
- Neutrino from accelerator

- Proton decay search
- **Indirect WIMP search**

Solar Neutrino measurement at Super-K

$$\nu + e^- \rightarrow \nu + e^- \text{ (elastic scattering)}$$

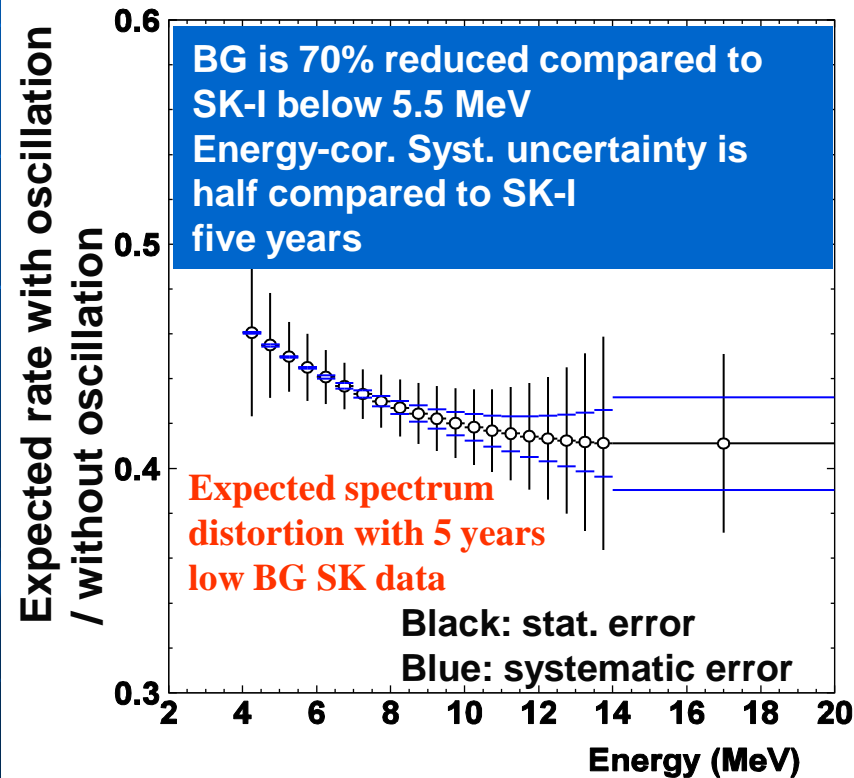
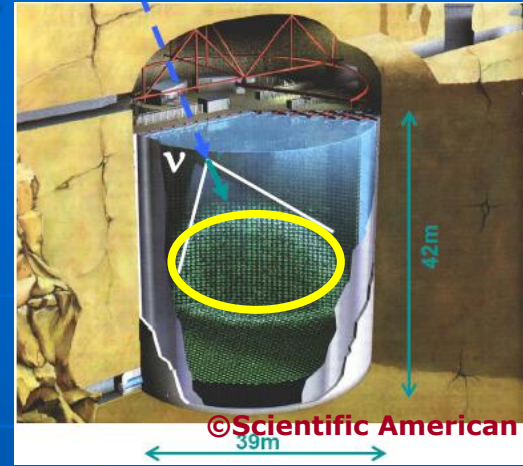
- Measure Cherenkov ring pattern from recoiled electron

- Timing information -> Vertex of interaction
- Hit pattern -> Direction
- # of hit PMTs -> Energy

- High statistics for ^8B neutrino (~ 15 events/day for $E_e > 5\text{MeV}$)
- good angular resolution

Goal:

- Precise measurement of the solar neutrino parameters (flux, timing variation, oscillation parameters etc)
- Reduce the b.g. level and measure the upturn in the solar neutrino spectrum .



2, Recent SK solar neutrino analysis

(SK-III phase)

<http://arxiv.org/abs/1010.0118>

Data set

SK-III period: **2006/8/5-2008/8/18**

(live time : 548 days, $E \geq 6.5$ MeV,
289 days, $E < 6.5$ MeV)

2006/8/5-2007/1/24 : 100%eff @6.5MeV

livetime 121.7 days

2007/1/24-2008/4/17 :100%eff @5.0MeV

livetime 331.5 days

(RR sample ❖ 210.7day)

2008/4/17-2008/8/18 : 100%eff @4.5MeV

livetime 94.8 days

(RR sample 87.5day)

❖RR sample : Radon Reduced sample for which high background rate periods are rejected from the normal run

Improvements in SK-III solar ν analysis

- Reduce Low energy BG ~70%
- Improved Systematics ~50%

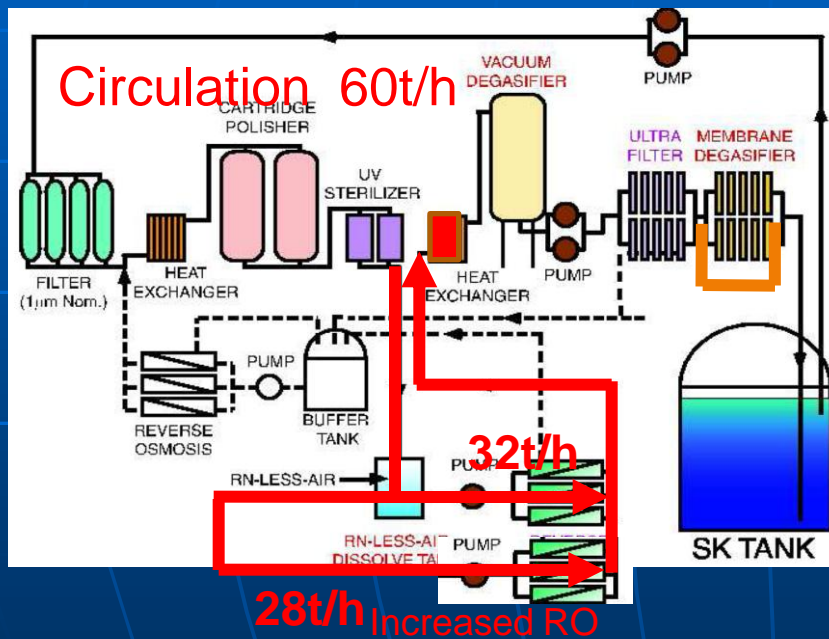
2-1, Reduction of background

Improvement of water circulation and purification system

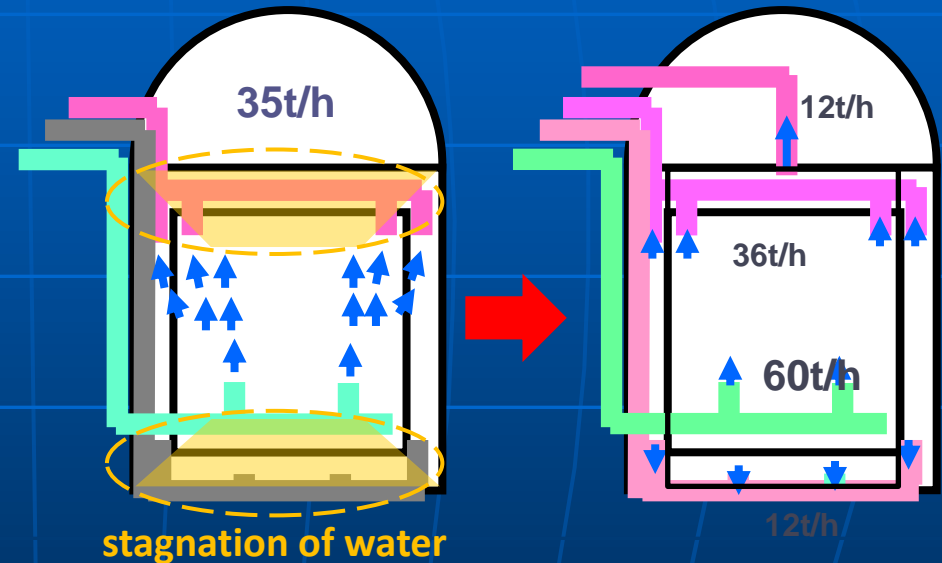
1, Improved water quality

Doubled circulation rate

Increased purification power

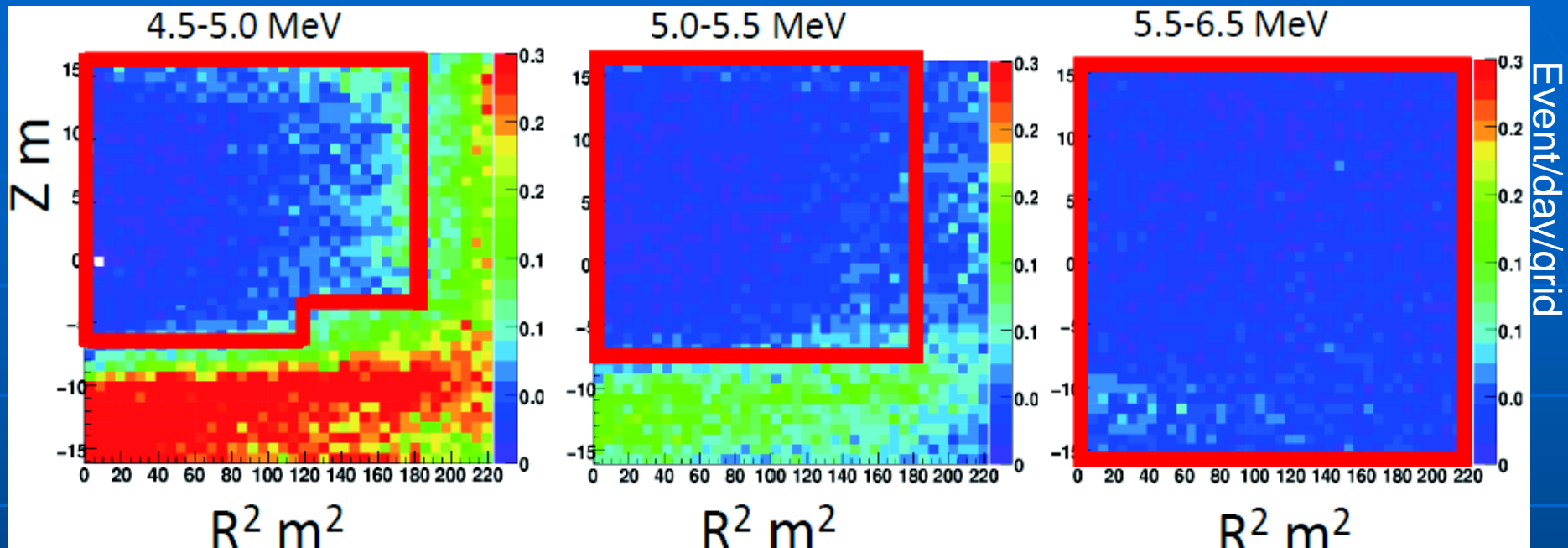


2, Optimized water flow in the tank



→ Lower Rn concentration in fiducial volume

Vertex distribution of final sample



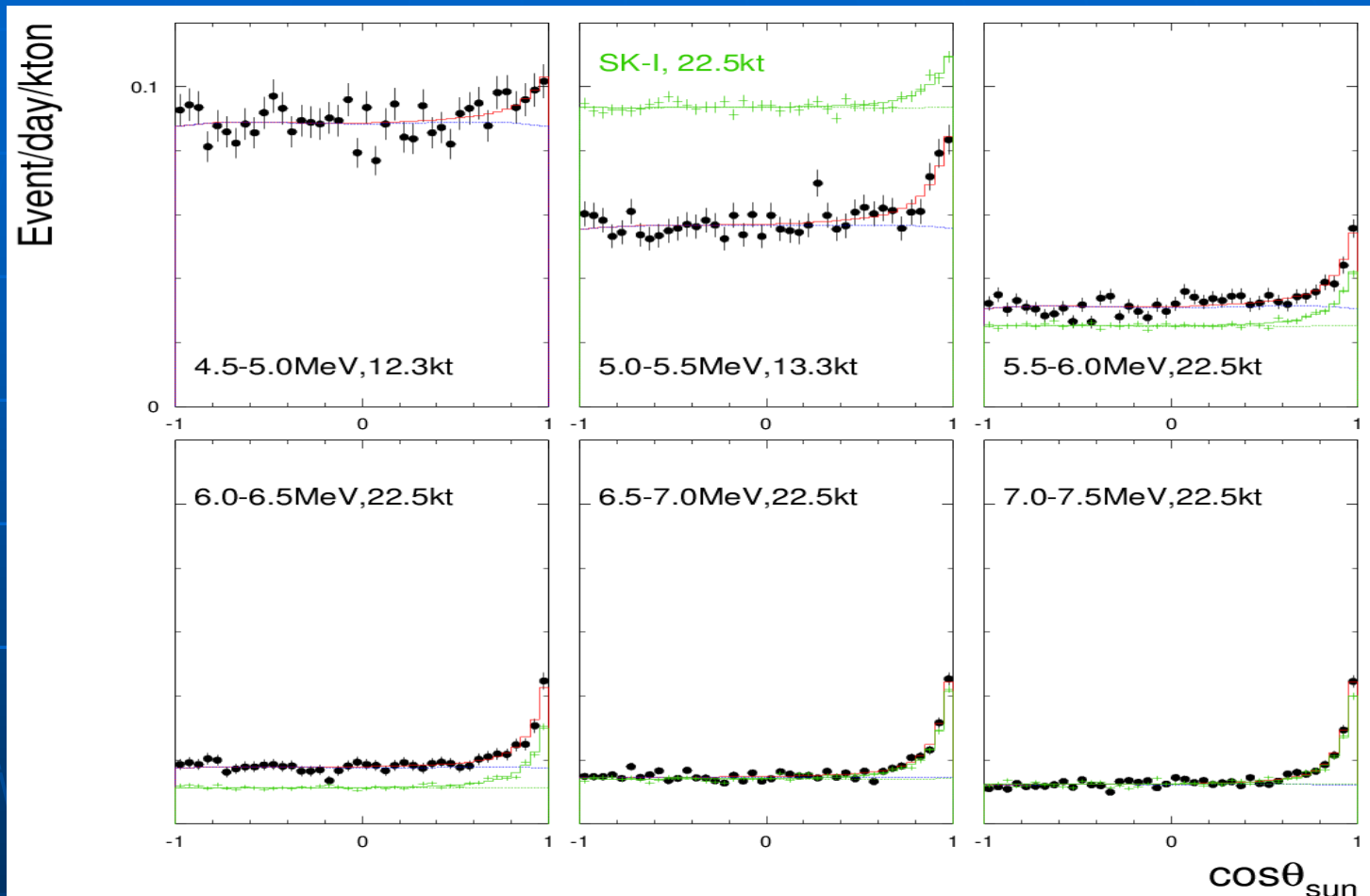
Fiducial volume of each energy region is shown as red box:
12.3kt (4.5-5MeV), 13.3kt(5-5.5MeV), and 22.5kt(5.5-20MeV)

With upgrade of water system, water with higher radioactivity stays near bottom region.

-> by applying tighter fiducial volume cut, low b.g. rate can be achieved for 4.5-5.5MeV region

Comparison of background rate between SK-I and III

Solar angular distribution for each energy range.



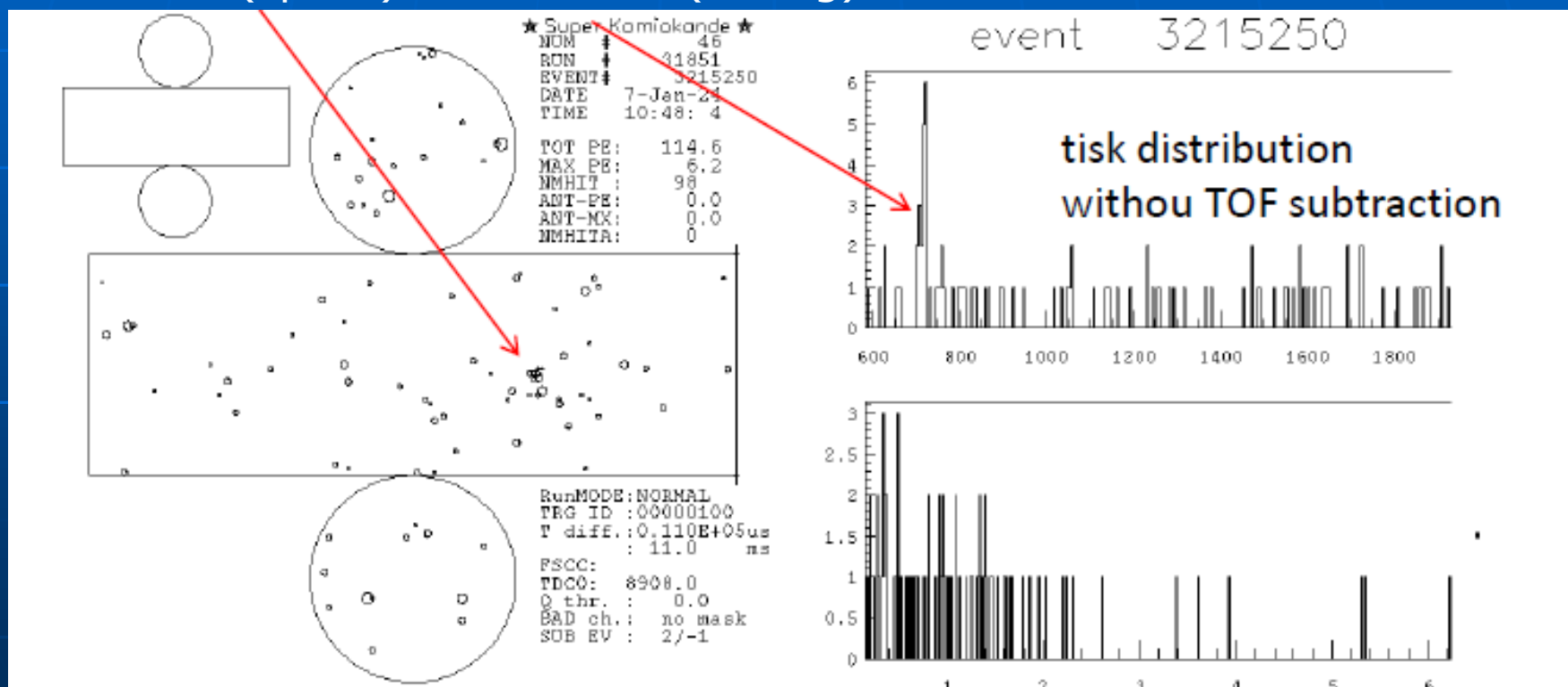
In lower energy region with tighter fiducial volume cut, SK-III has a lower b.g. rate due to lower radon concentration in water around the central region of the detector.

New cut for low energy events

Background events coming from radioactive sources in FRP cover of PMTs or wall have small clusters in space and timing distribution, when compared with neutrino events near the wall.

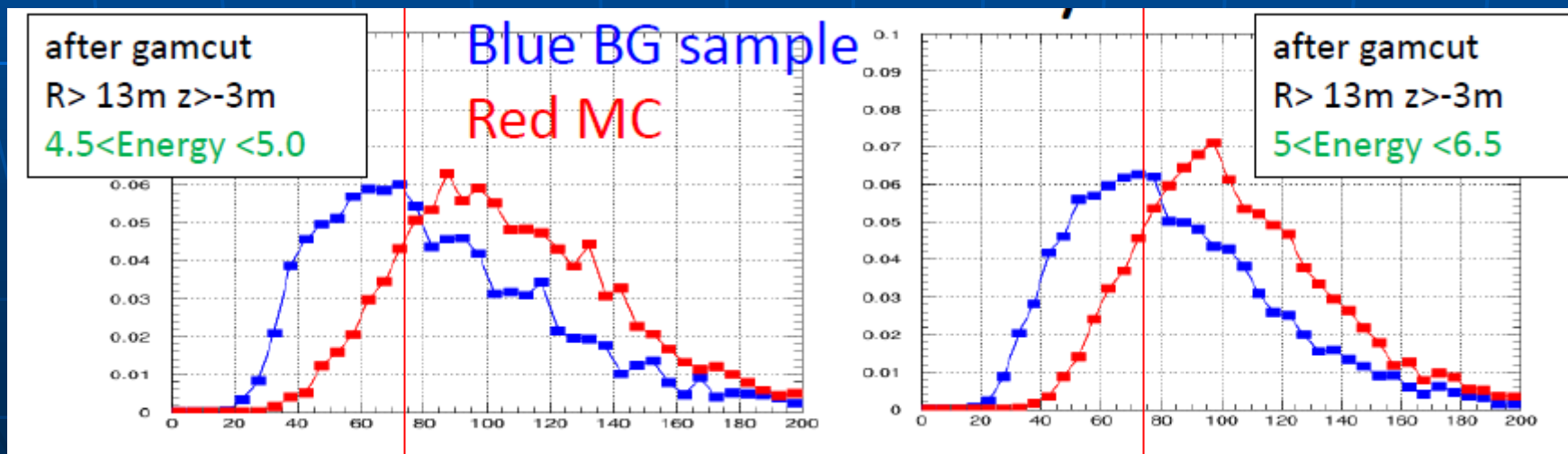
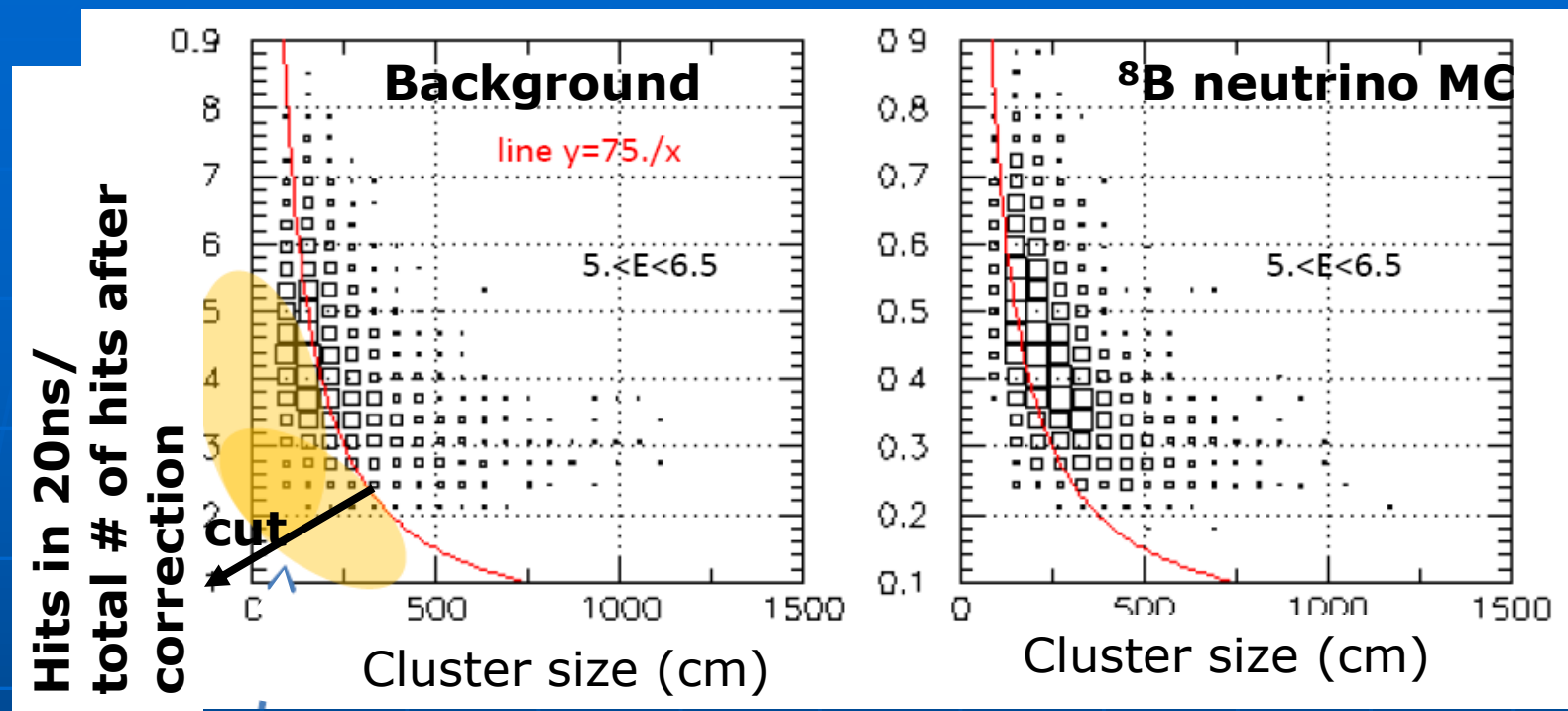
Cluster(space)

Cluster(timing)



-> Use variables related with cluster size for b.g. reduction.

New cut for low energy events(cont'd)



Horizontal axis : Cluster size * concentration in timing distribution

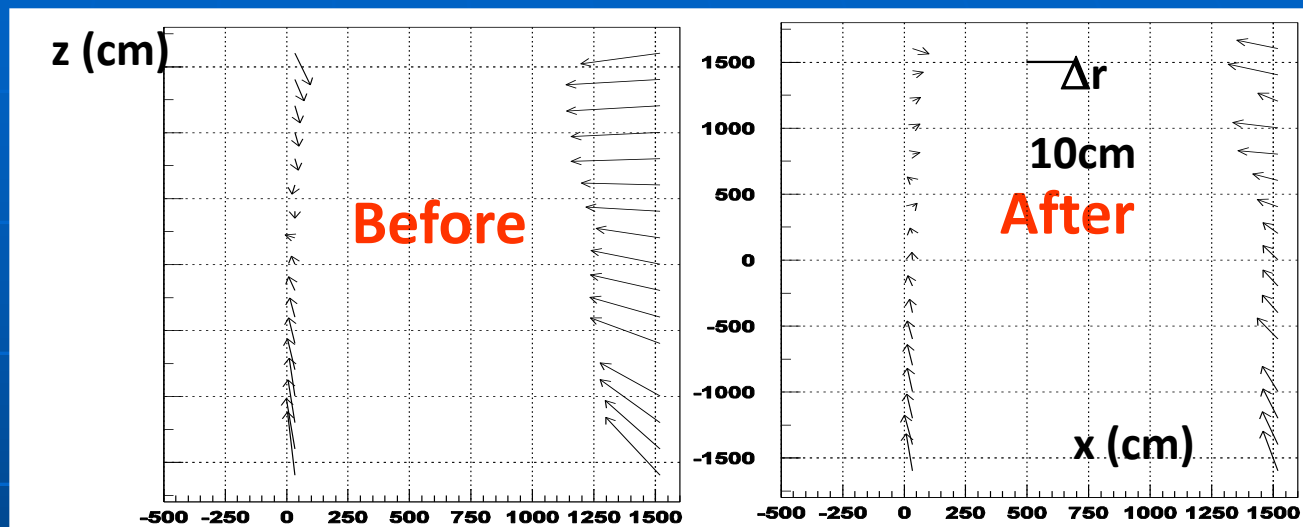
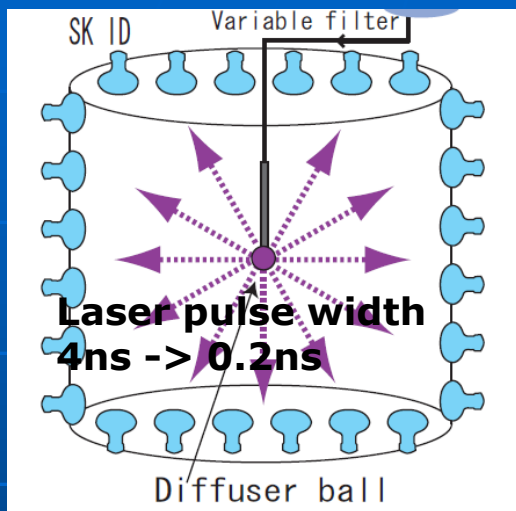
2-2, Improved systematics

Timing Calibration improvement

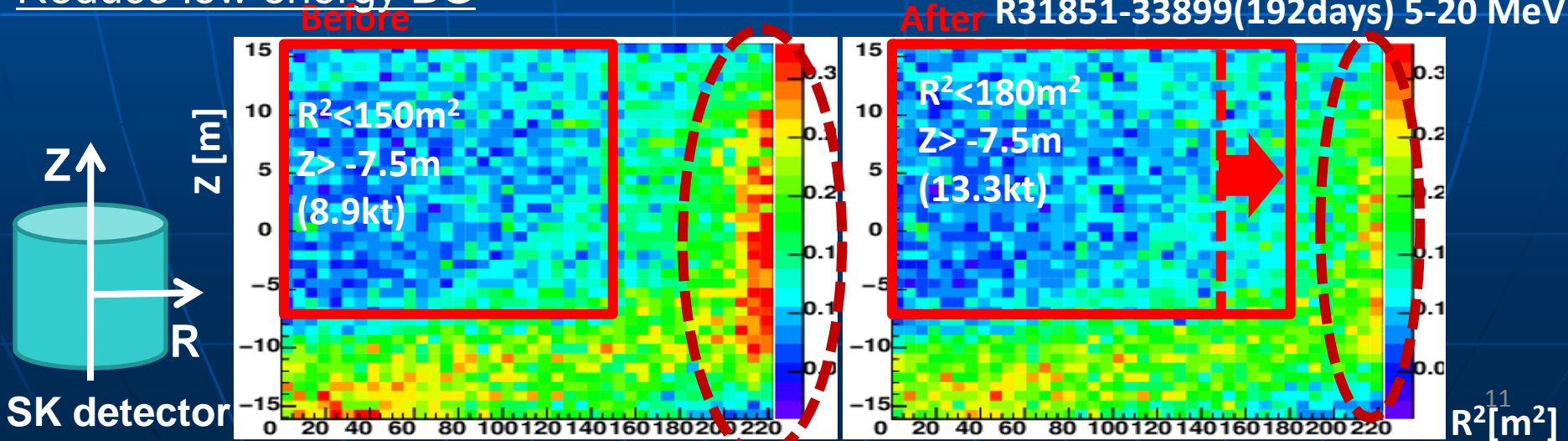
New hit timing correction is installed.

Electronics linearity is corrected by this correction

Improve systematics (vertex shift)

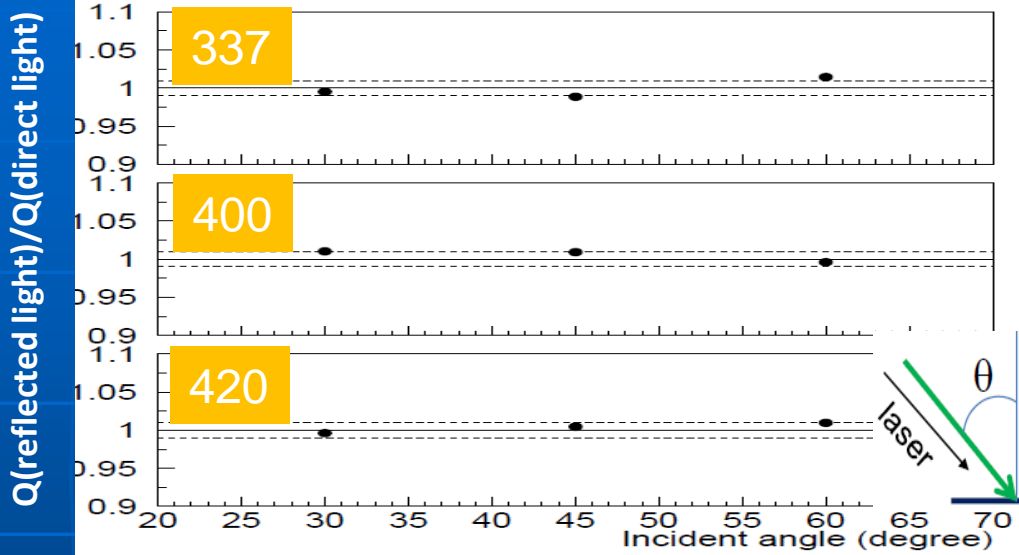


Reduce low energy BG

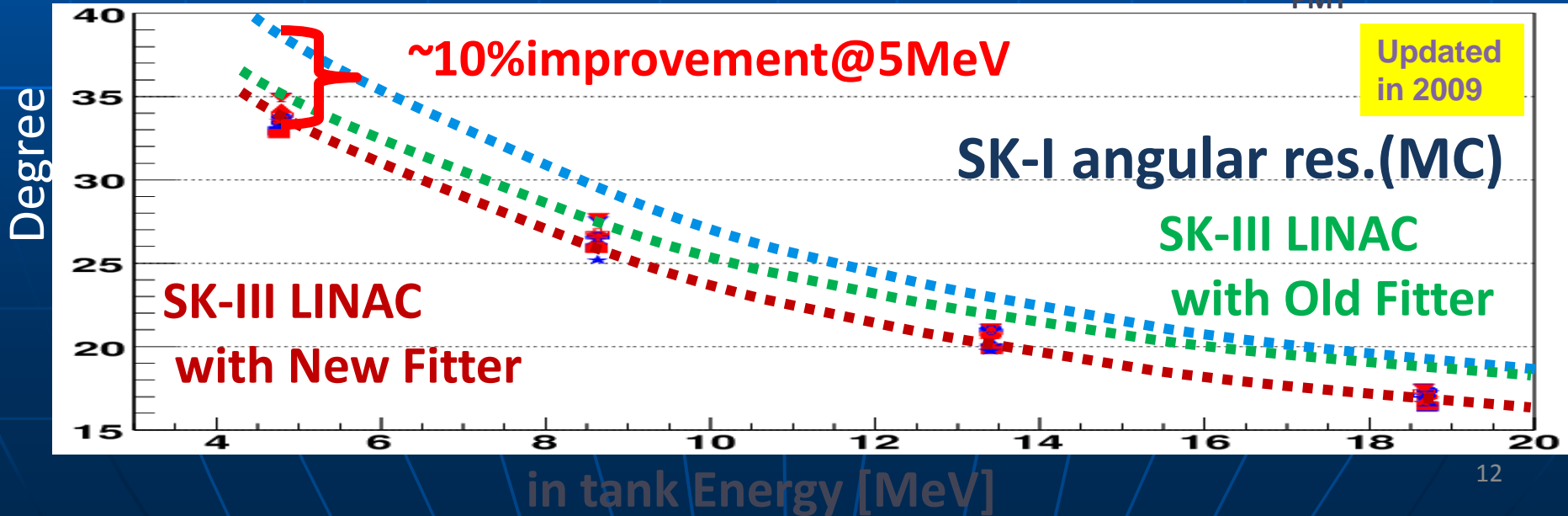
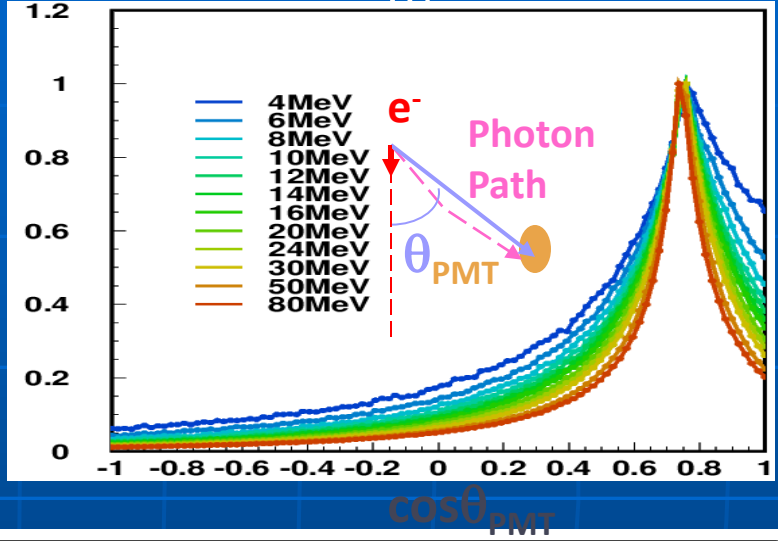


Angular reconstruction

Calibration&MC tuning:
black sheet reflectivity

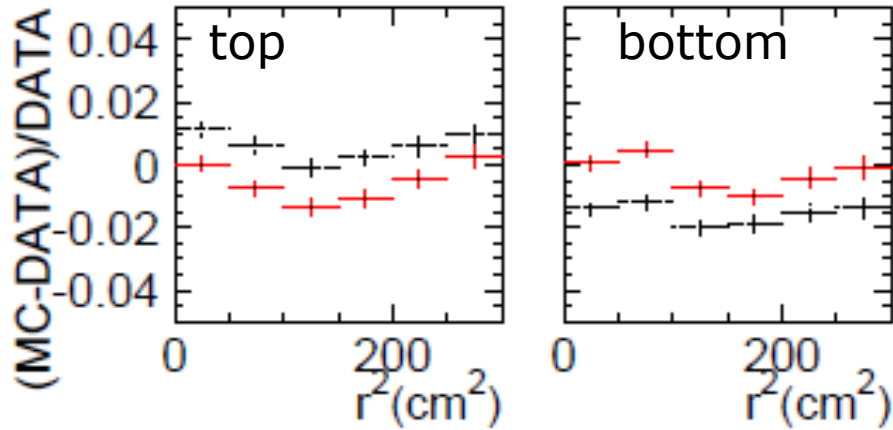
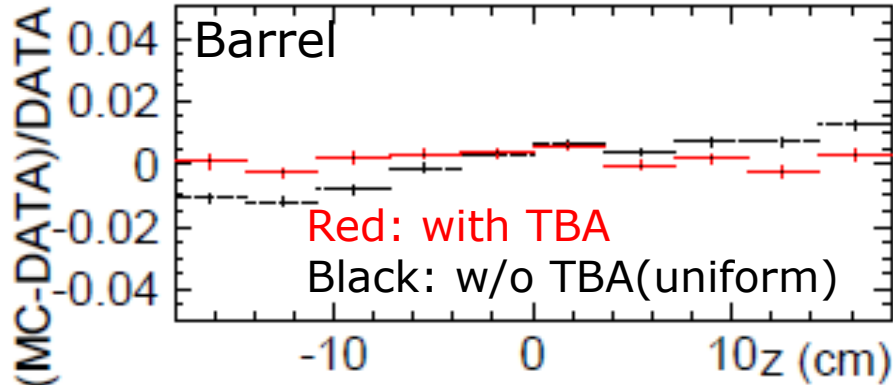


Improving direction fitter
Made likelihood functions
for different energy bins from MC



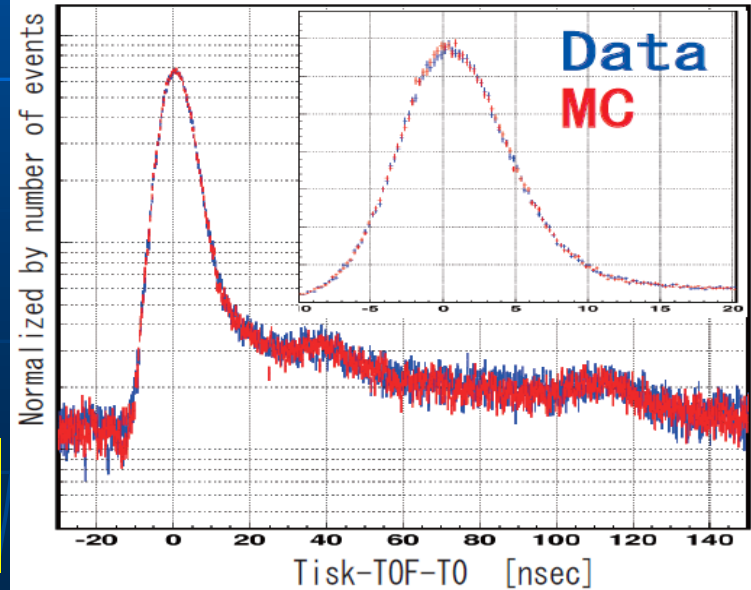
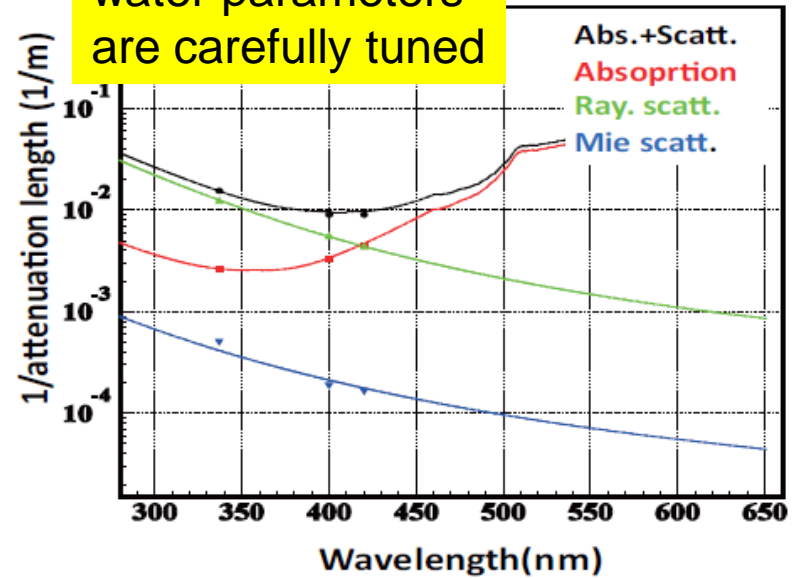
MC improvement

Top-bottom asym.(TBA) parameter is newly installed in SK-III MC's water transparency parameters

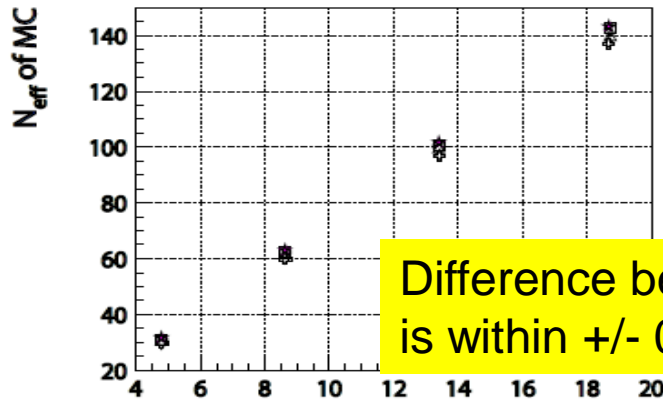
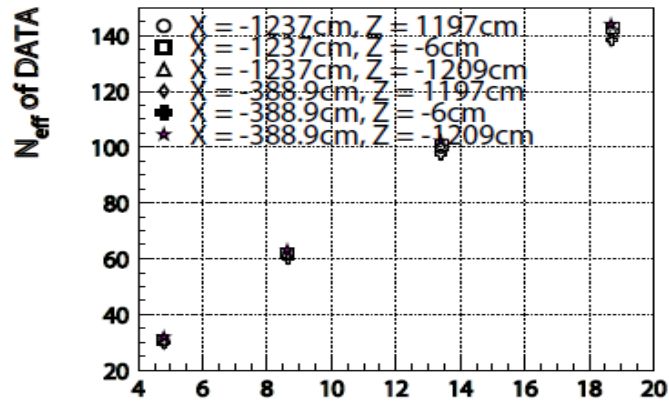
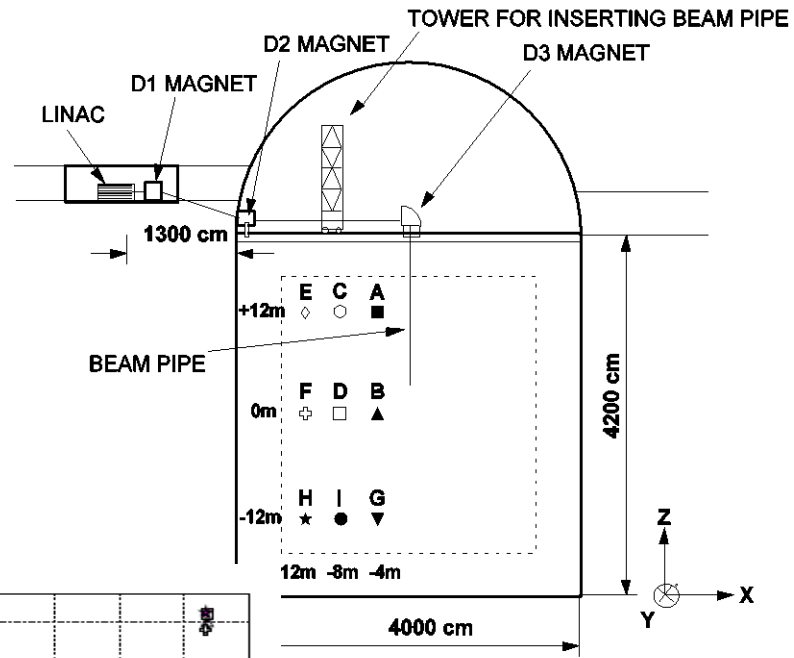


MC hit timing distribution of LINAC is perfectly matched to DATA

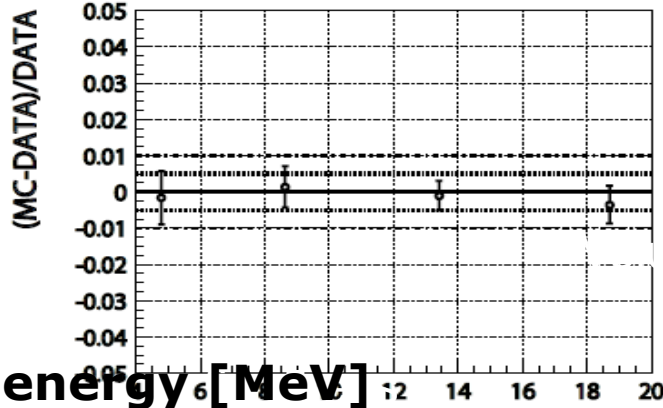
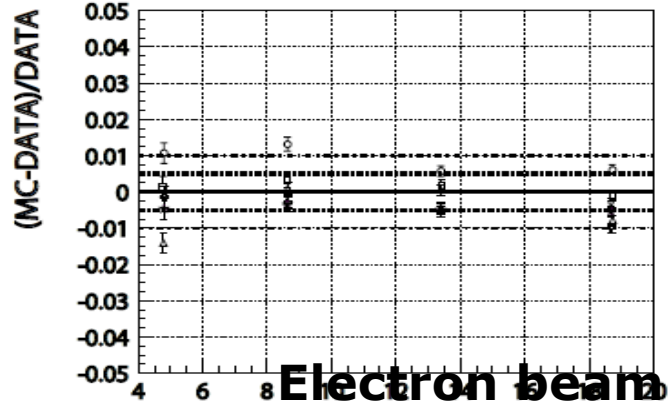
water parameters are carefully tuned



Energy scale



Difference between MC and DATA is within +/- 0.5%



Electron beam energy [MeV]

expected energy in tank

me average

Table of systematic uncertainties

	SK-III (Preliminary)	SK-I
Energy scale	+/-1.4	+/-1.6
Energy resolution	+/-0.2	
8B spectrum shape	+/-0.2	+1.1/-1.0
Trigger efficiency	+/-0.5	+0.4/-0.3
Vertex shift	+/-0.54	+/-1.3
Reduction	+/-0.65	+2.1/-1.6
Small cluster hits cut	+/-0.5	
Spallation cut	+/-0.2	+/-0.2
External event cut	+/-0.25	+/-0.5
Background shape	+/-0.1	+/-0.1
Angular resolution	+/-0.67	+/-1.2
Signal extraction method	+/-0.7	
Cross section	+/-0.5	+/-0.5
Live time calculation	+/-0.1	+/-0.1
Total	+/-2.1	+3.5/-3.2%

Timing calibration

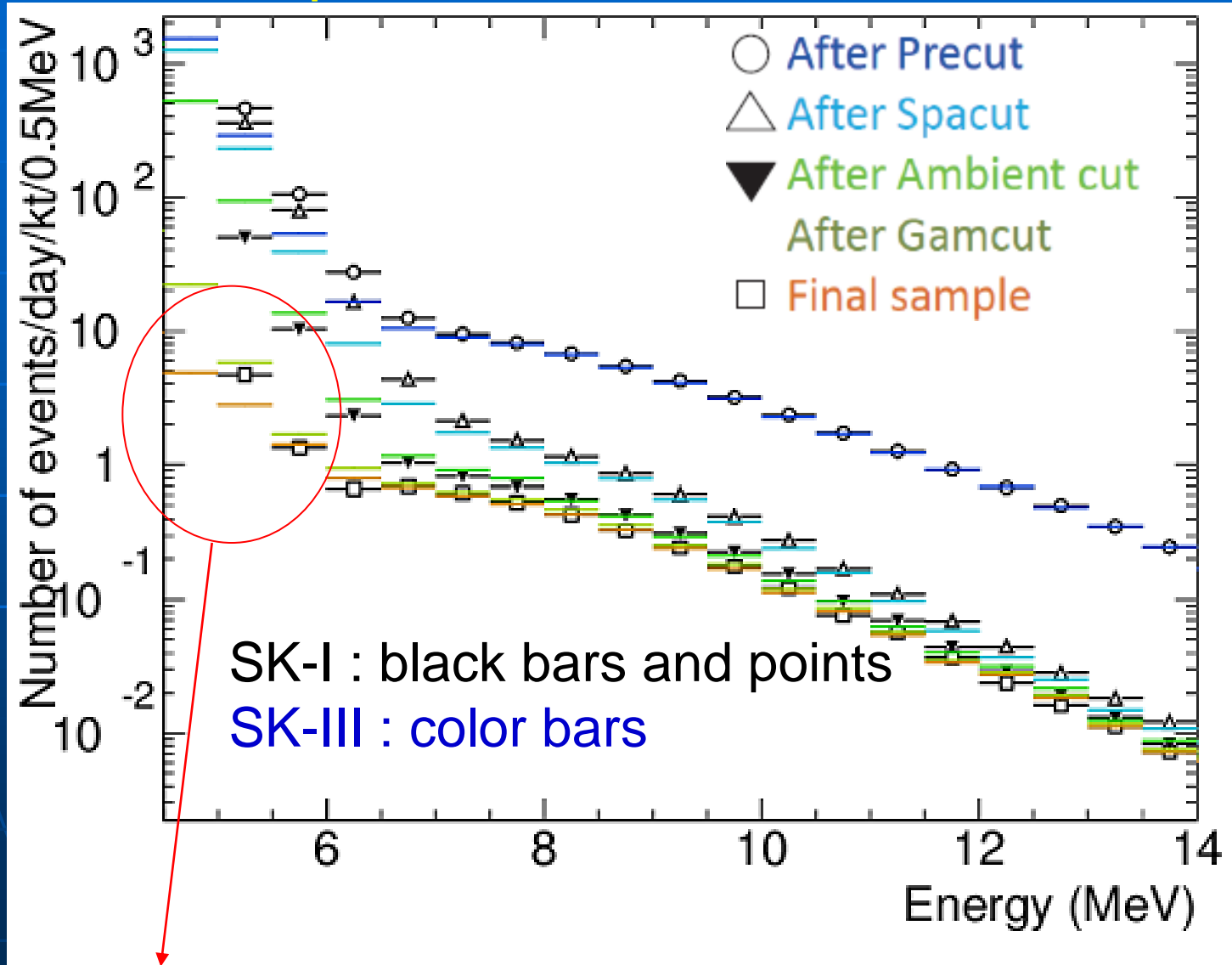
Improvement of
reduction tools
and MC

Improvement
Direction fitter

Due to Improvement of
detector MC, reconstruction
tools and calibration,
systematic errors
were reduced
from +3.5/-3.2%(SK-I)
To +2.1%(SK-III). -> ~60%

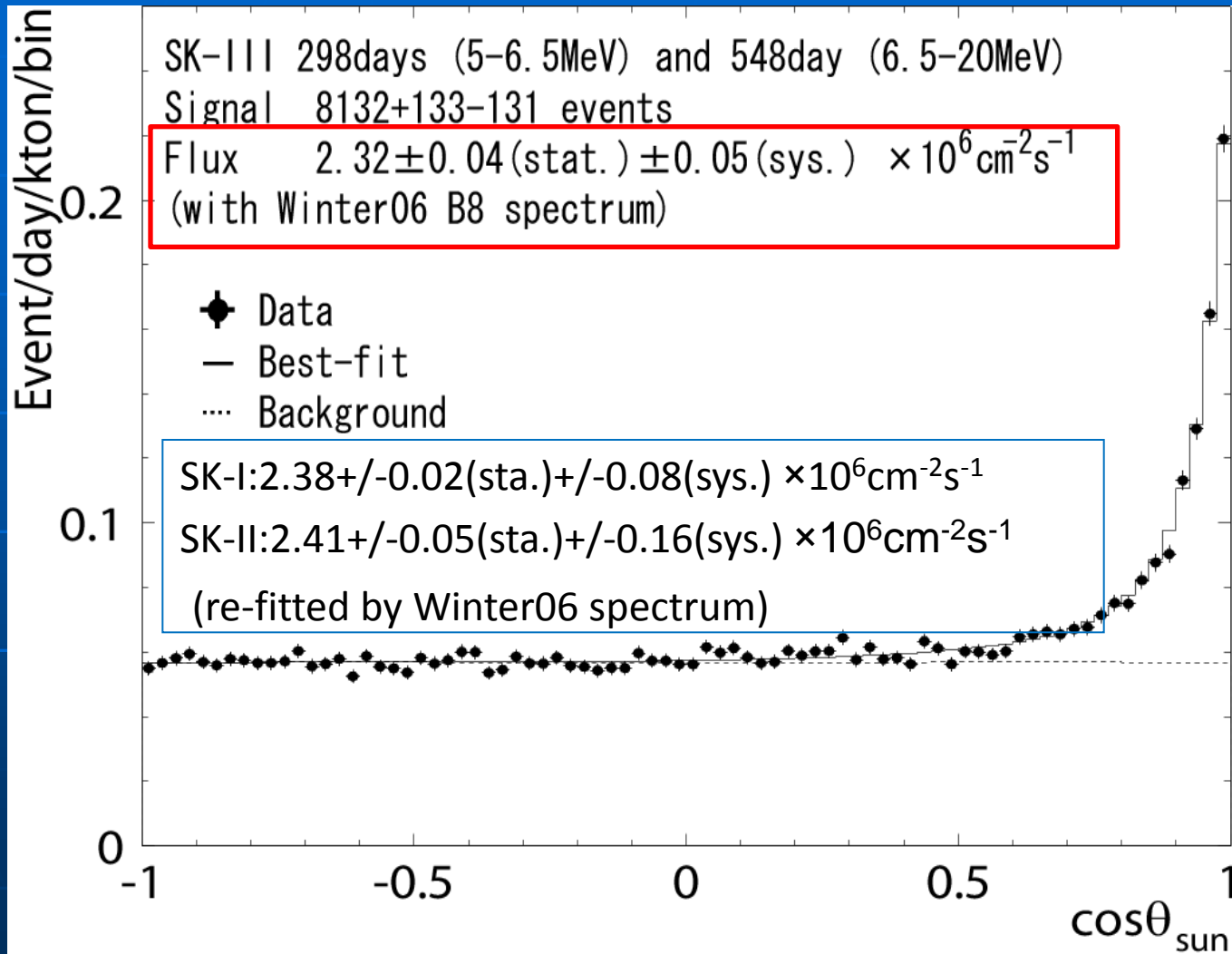
3, Solar neutrino results in SK-III

Reduction step



For lower energy region, SK-III has lower b.g. level than SK-I.

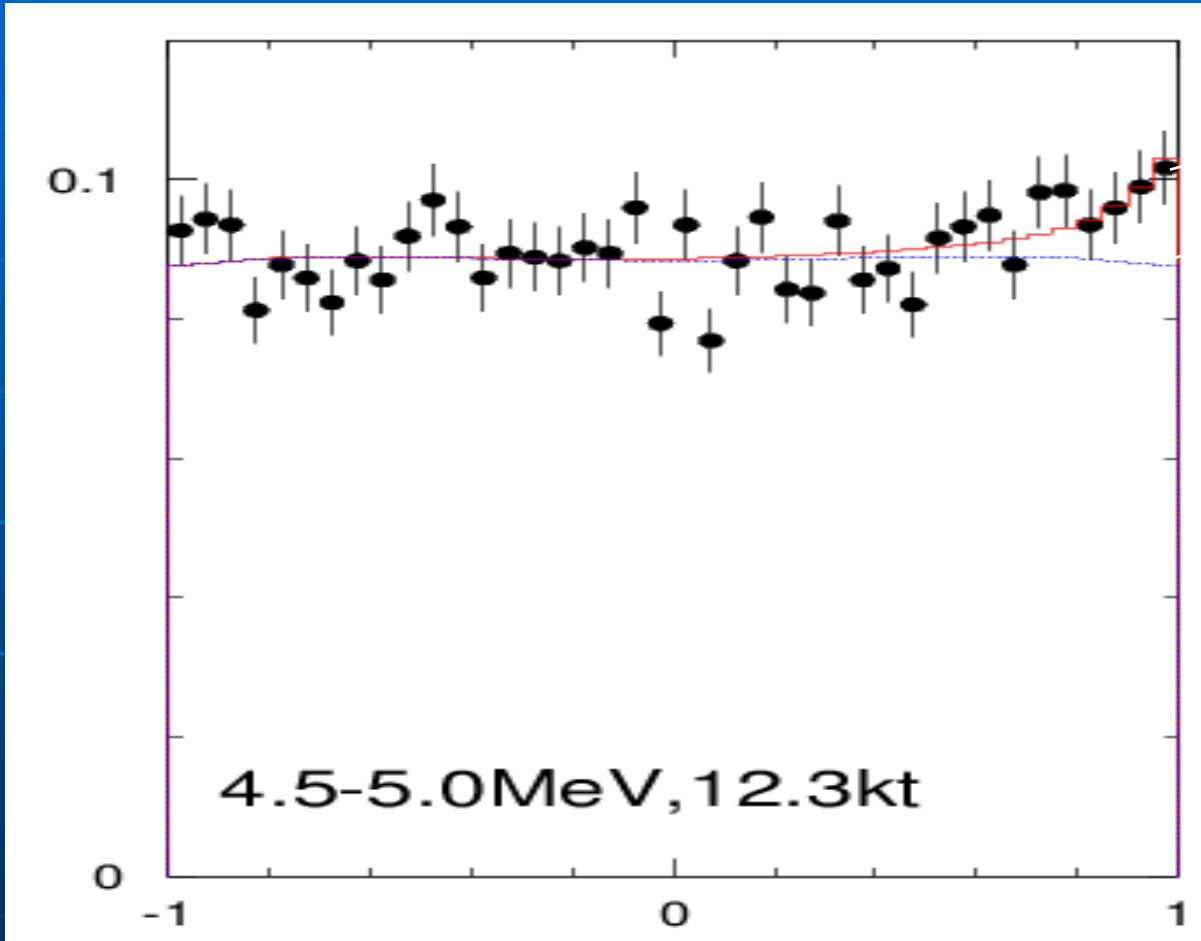
Solar neutrino flux for E=5-20MeV



- SK-III result is Consistent with SK-I and II.

- Systematic error is reduced.

Angular distribution for E=4.5-5.0MeV



RED: best fit curve

Blue: back ground

For 4.5-5.0MeV region,

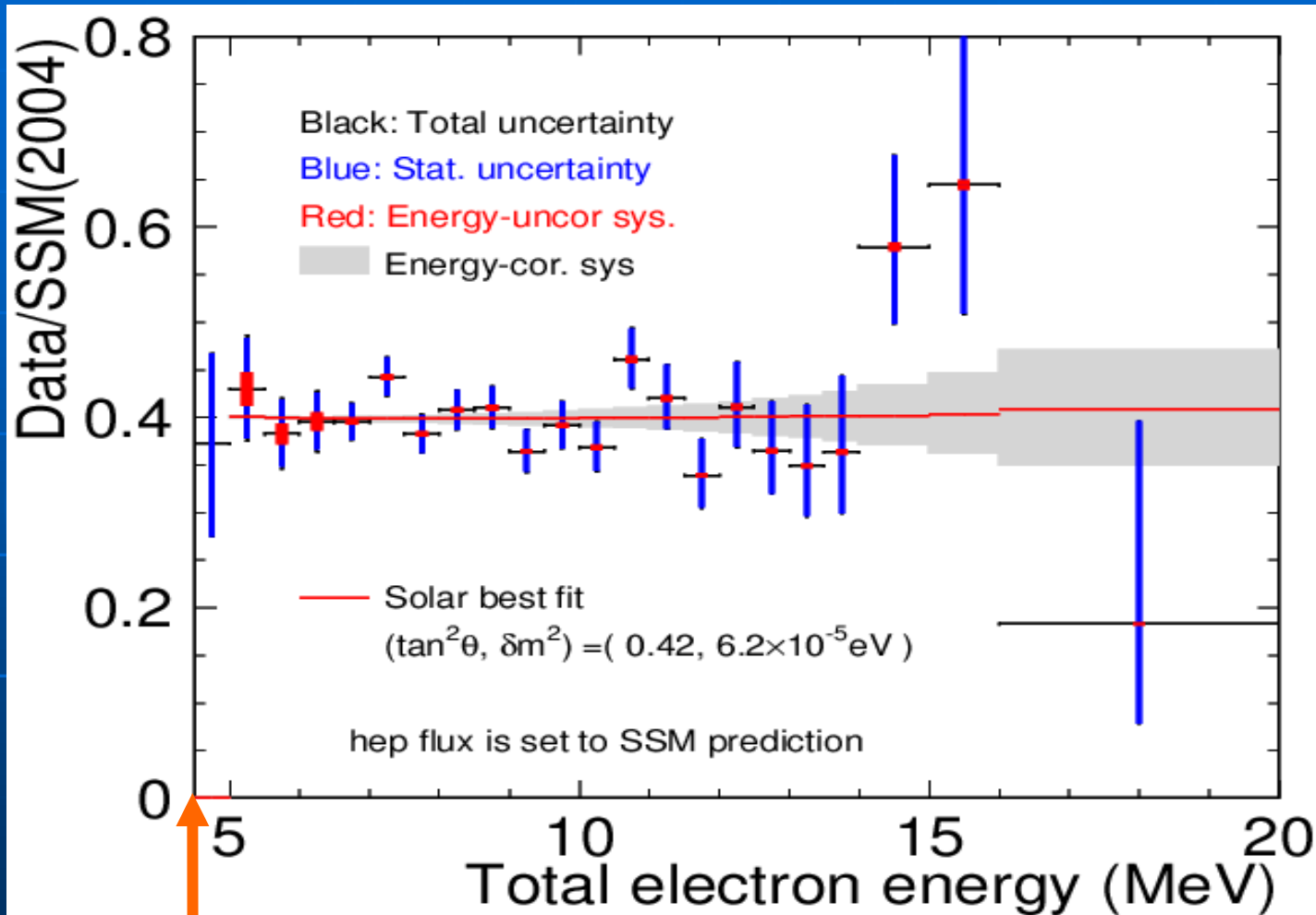
232. \pm 59. event

2.14 + 0.54-0.54(stat.)

$\times 10^6 \text{cm}^{-2} \text{sec}^{-1}$

Solar neutrino in this energy region was measured with 4σ significance.

^8B Energy spectrum of SK-III data

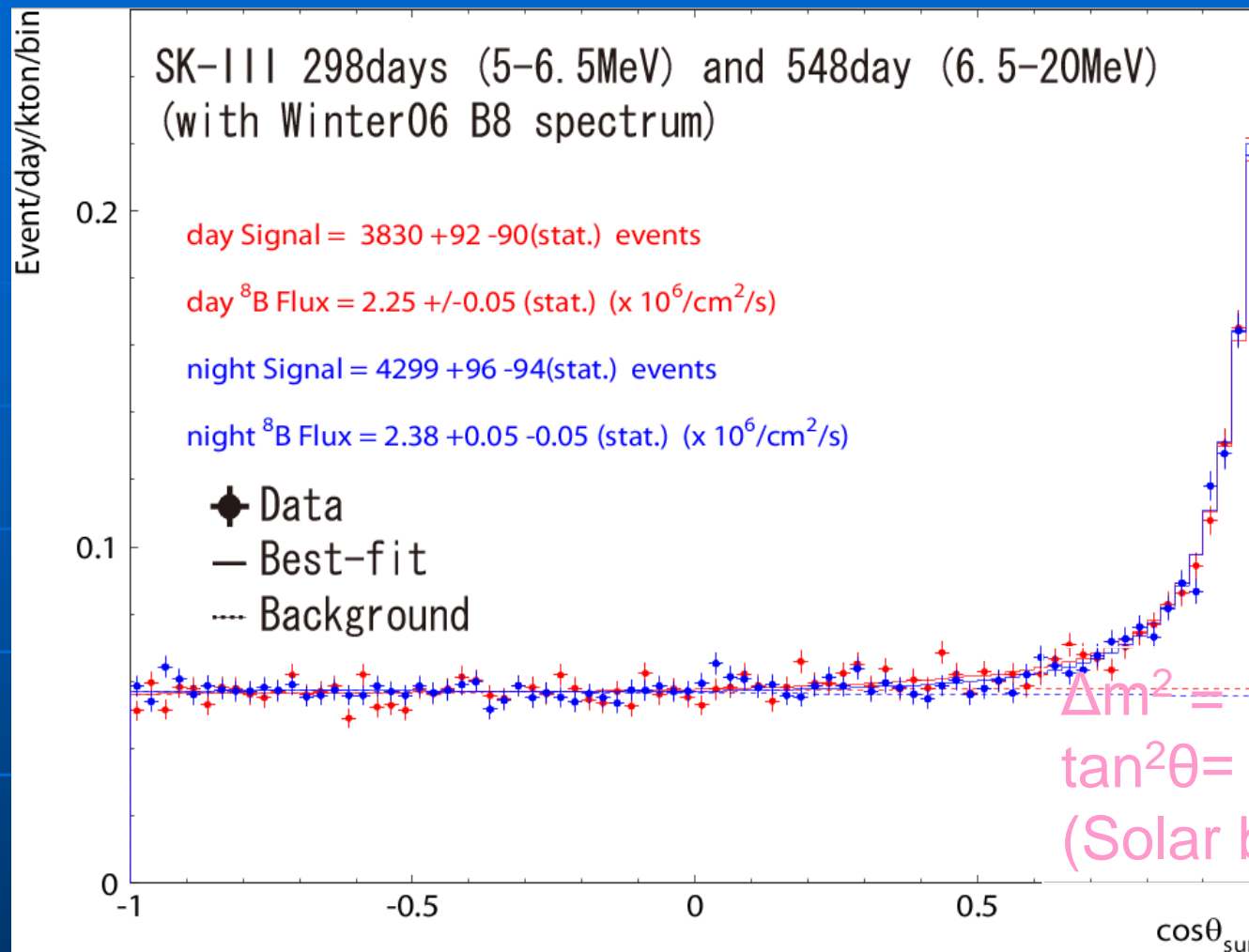


4.5 MeV (total energy)
4.0 MeV (kinetic energy)

Consistent with

- SK-I result
- No distortion

Day/Night flux



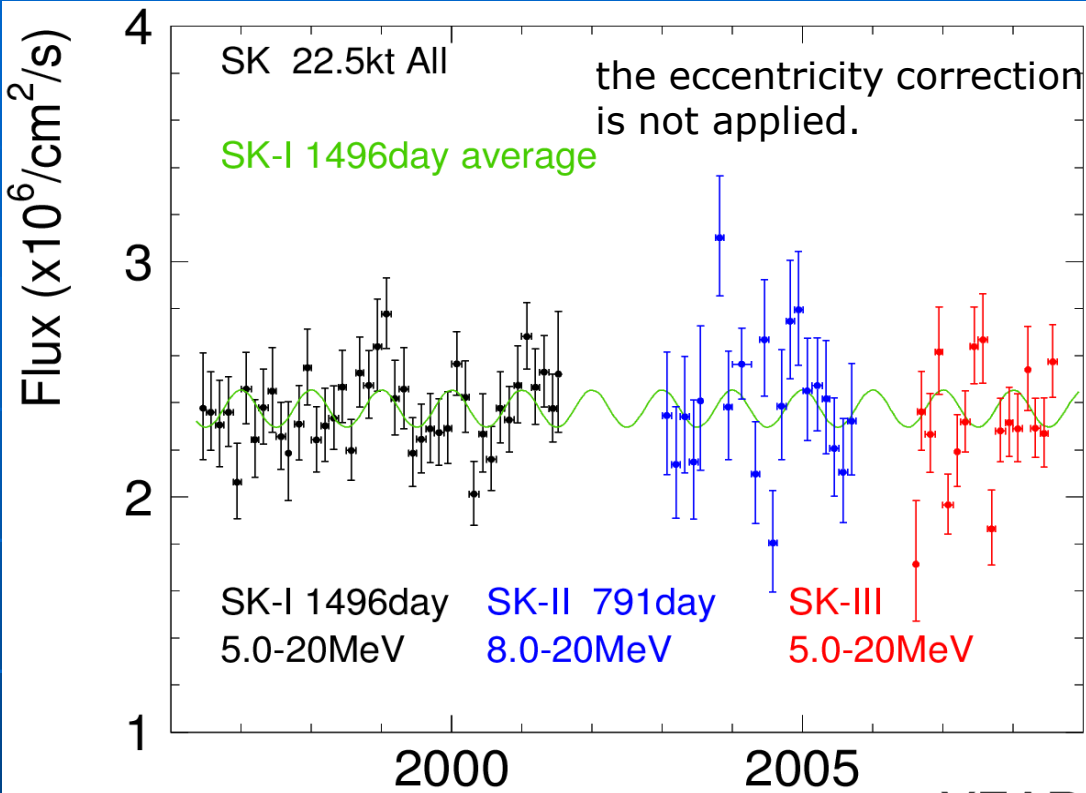
$$\text{SK-I: } A_{\text{DN}} = -1.8 \pm 1.6 \quad {}^{+1.3}_{-1.2} \%$$

$$\text{SK-II: } A_{\text{DN}} = -3.6 \pm 3.5 \pm 3.7 \%$$

$$\text{SK-III: } A_{\text{DN}} = -4.1 \quad {}^{+2.5}_{-2.6} \pm 1.3 \%$$

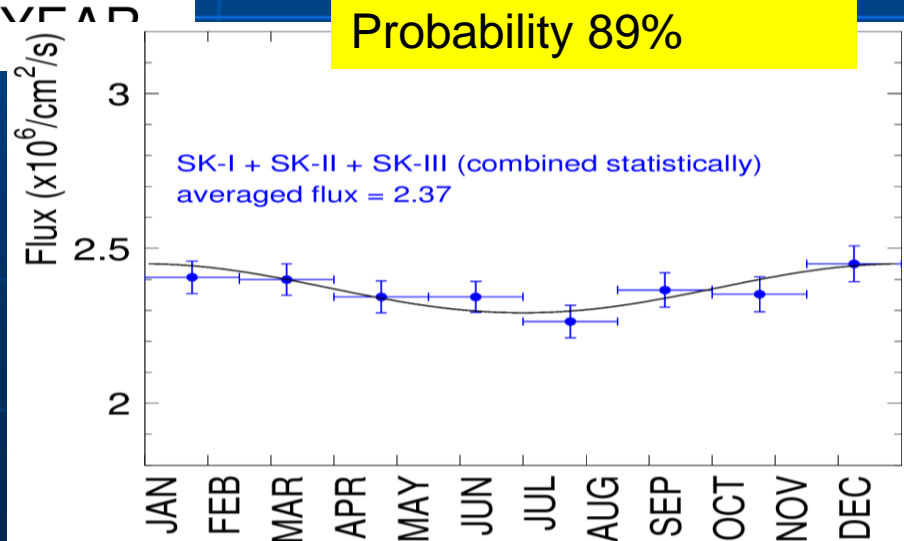
combined: $A_{\text{DN}} = -2.3 \pm 1.3 \%$ (stat) sys : under study

Seasonal variation



SK-I,II,III
 $\chi^2 = 3.6$
 (only stat)
 With dof = 7
 Probability 89%

Consistent with the eccentricity of the orbit ←



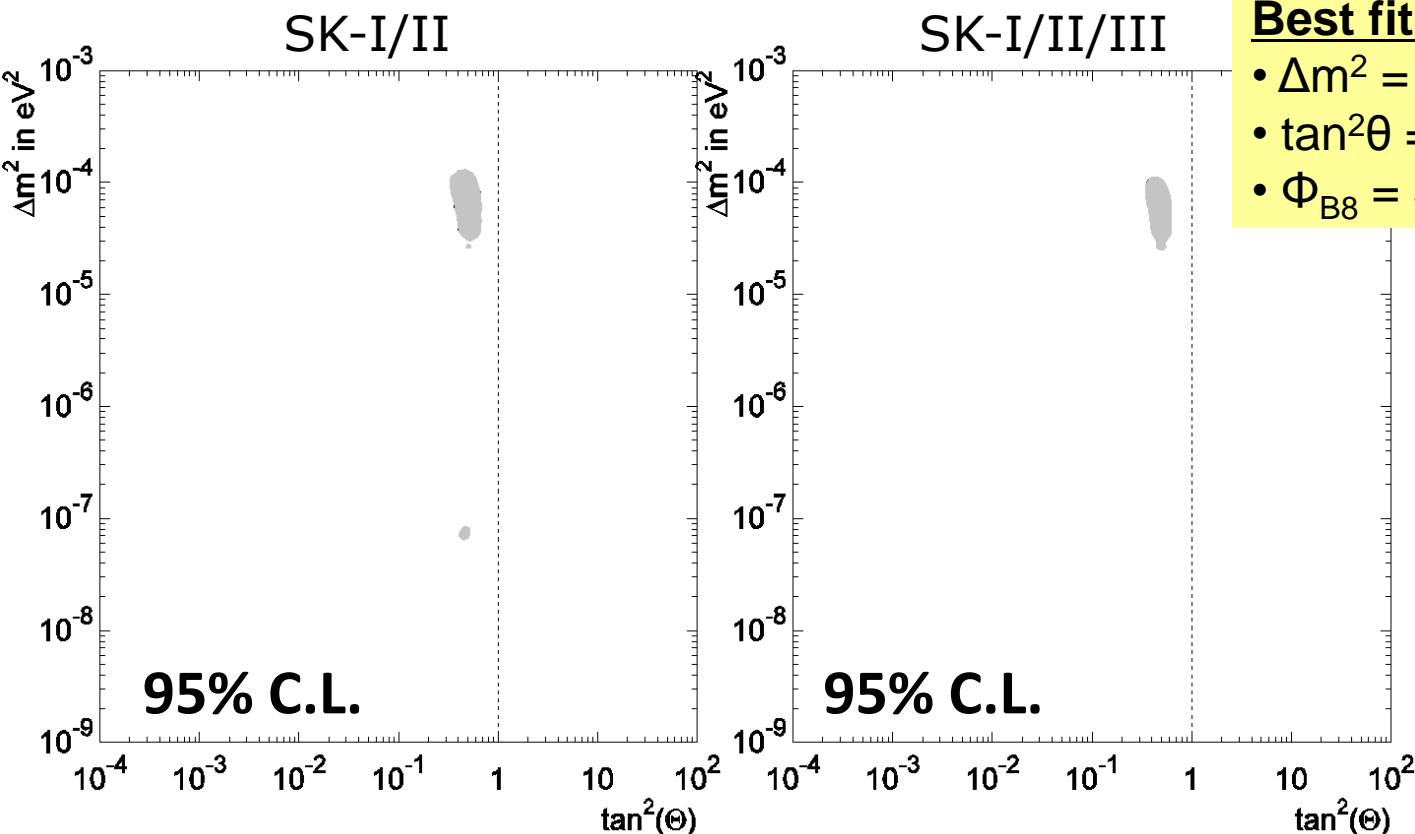
4, Oscillation results

2-flavor SK-I/II/III with flux constraint

- SK-I 1496 days, spectrum 5.0-20MeV + D/N : $E \geq 5.0\text{MeV}$
- SK-II 791 days, spectrum 7.0-20MeV + D/N : $E \geq 7.5\text{MeV}$
- **SK-III 548 days, spectrum 5.0-20.0MeV + D/N : $E \geq 5.0\text{MeV}$**

B8 rate is constrained by SNO(NCD+LETA) NC flux = $(5.14 \pm 0.21) 10^6 \text{cm}^{-2}\text{s}^{-1}$

Hep is constrained by SSM flux with uncertainty(16%)



Best fit value (preliminary)

- $\Delta m^2 = 6.1 \times 10^{-5} \text{ eV}^2$
- $\tan^2 \theta = 0.48$
- $\Phi_{B8} = 5.2 \times 10^6 \text{ cm}^{-2}\text{s}^{-1}$

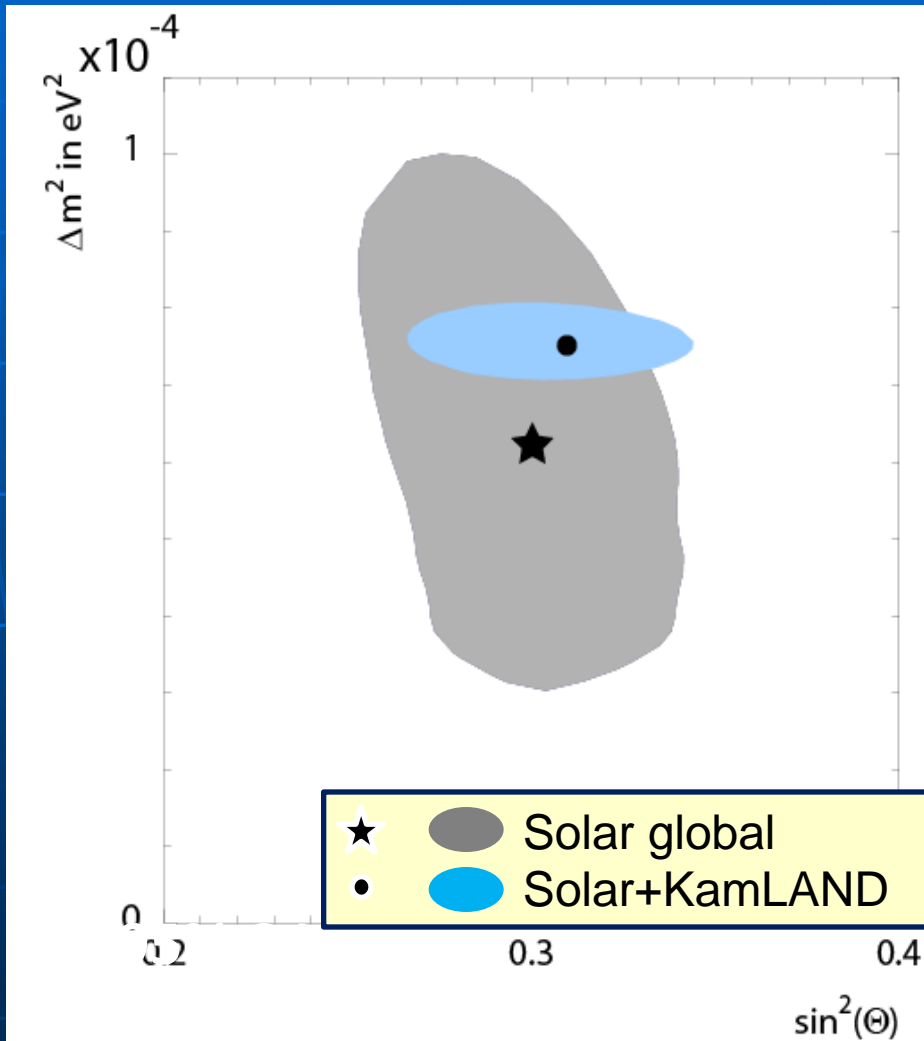
**Only LMA
(i.e. LOW
excluded)**

Global oscillation analysis

Data set

- SK-I/II/III
- SNO : CC flux(Phase-I & II & III)
NC flux(Phase-III & LETA combined)
(= $(5.14 \pm 0.21) 10^6 \text{cm}^{-2}\text{s}^{-1}$)
Day/Night asymmetry(Phase-I & II)
- Radiochemical : Cl, Ga
 - New Ga rate: 66.1 ± 3.1 SNU (All Ga global)
(Phys.Rev.C80:015807,2009.)
 - Cl rate: 2.56 ± 0.23 (Astrophys. J. 496 (1998) 505)
- Borexino
 - ^7Be rate: 48 ± 4 cpd/100tons
(PRL 101: 091302, 2008)
- KamLAND : 2008

2-flavor global analysis



Best fit value (preliminary)

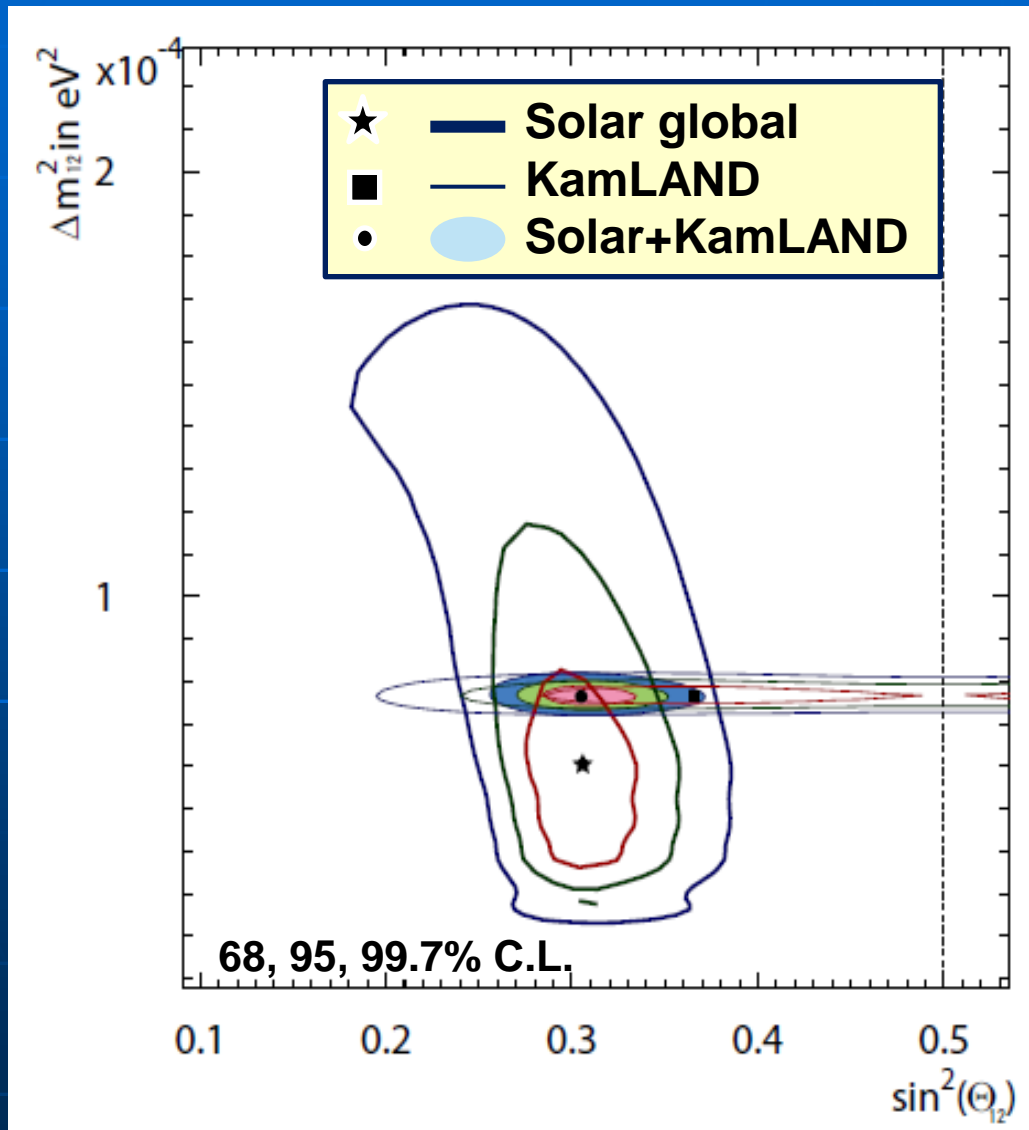
Solar global

- $\Delta m^2 = 6.2 \times 10^{-5} \text{ eV}^2$
- $\tan^2 \theta = 0.48$
- $\Phi_{B8} = 5.3 \pm 0.2 \times 10^6 \text{ cm}^{-2} \text{ s}^{-1}$

Solar global + KamLAND

- $\Delta m^2 = 7.6 \times 10^{-5} \text{ eV}^2$
- $\tan^2 \theta = 0.3$
- $\Phi_{B8} = 5.1 \pm 0.1 \times 10^6 \text{ cm}^{-2} \text{ s}^{-1}$

3-flavor global analysis: $\theta_{12} - \Delta m_{12}^2$



Free parameters :
 $\theta_{12}, \theta_{13}, \Delta m_{12}^2$

Best fit value (preliminary)

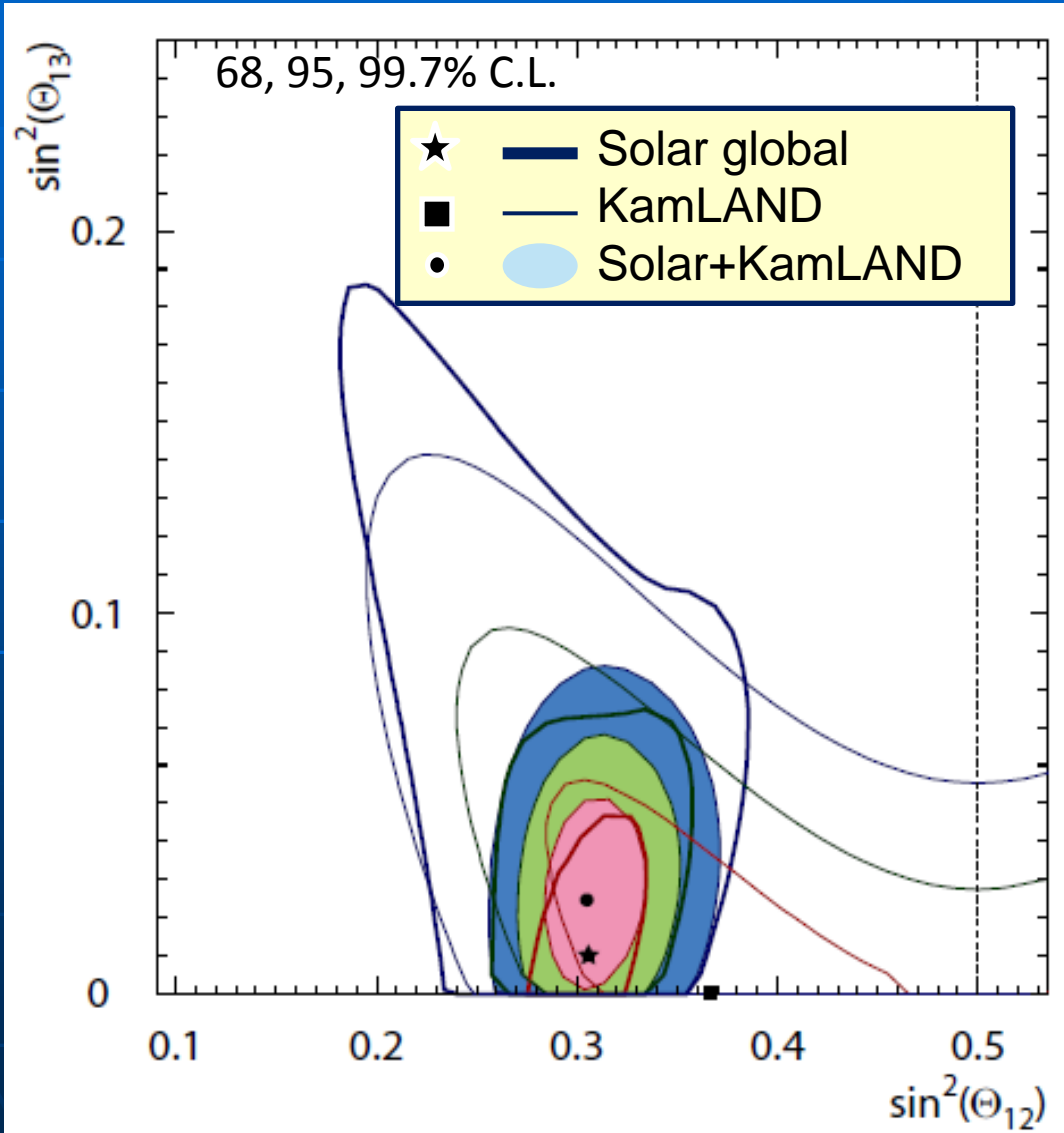
Solar global

- $\Delta m^2 = 6.2 \times 10^{-5} \text{ eV}^2$
- $\sin^2 \theta_{12} = 0.31$
- $\sin^2 \theta_{13} = 0.010$
- $\Phi_{B8} = 5.3 \pm 0.2 \times 10^6 \text{ cm}^{-2} \text{ s}^{-1}$

Solar global+KamLAND

- $\Delta m^2 = 7.7 \times 10^{-5} \text{ eV}^2$
- $\sin^2 \theta_{12} = 0.31$
- $\sin^2 \theta_{13} = 0.025 \begin{matrix} +0.018 \\ -0.016 \end{matrix}$
- $\Phi_{B8} = 5.3 + 0.1 - 0.2 \times 10^6 \text{ cm}^{-2} \text{ s}^{-1}$

3-flavor global analysis: $\theta_{12} - \theta_{13}$



Solar global

$\sin^2\theta_{13} < 0.060$
@95% C.L.

Solar global + KamLAND

$\sin^2\theta_{13} < 0.059$
@95% C.L.

5, SK-IV status

1, SK-IV Electronics and DAQ system were updated at the beginning of SK-IV phase)

Improvements of front-end electronics

- 5 times wider dynamic range for charge measurement ($>2000\text{pC}$)
- **Larger amount of data can be sent to Online system via 100Base/T Ethernet**
- Low power consumption ($< 1\text{W/ch}$)

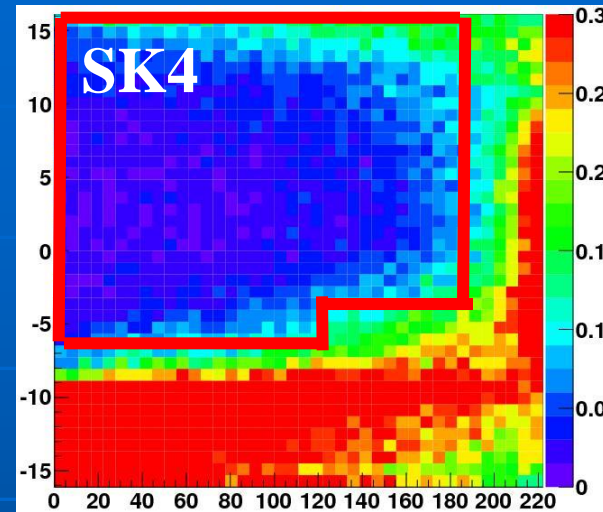
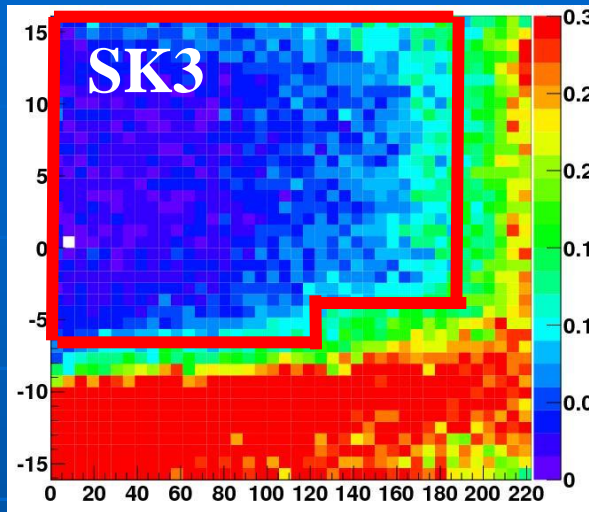
Improvements of online-DAQ system

- SK-I/II/III DAQ system
Hardware trigger was used. Only Triggered hit data was sent to online system.
- SK-IV system
All the hit data is sent to the online system and event building is done by software
-> capable of lower energy threshold

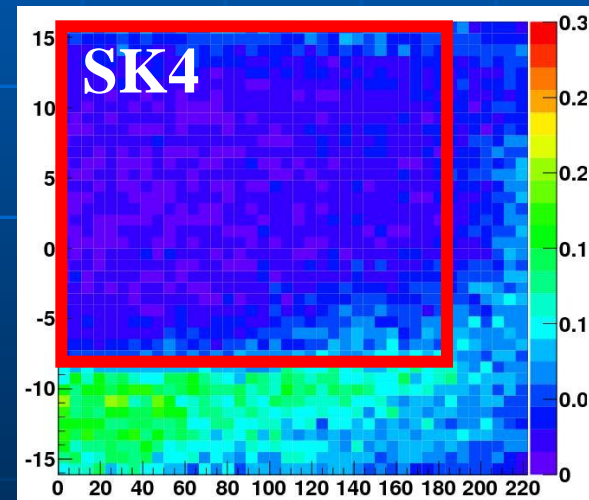
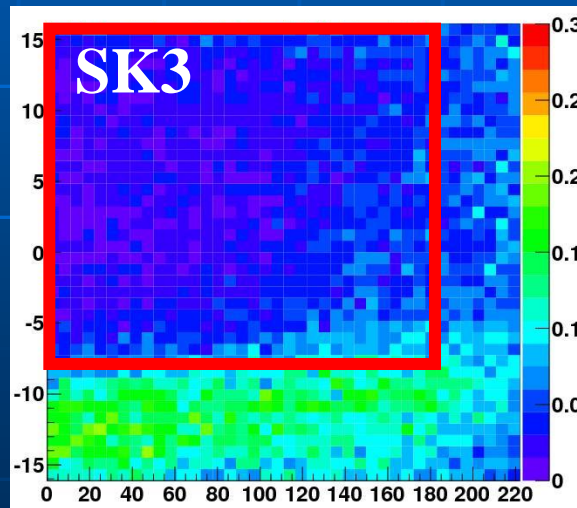
2, Fine water temperature control for inlet water -> Lower radon concentration in fiducial volume

Background level in SK-IV

4.5-5.0 MeV



5.0-5.5 MeV



Same level of b.g. level as SK-III have been achieved in SK-IV phase.

6, Summary

- Results of solar measurement in SK-III phase have been reported.
- There are improvements for b.g. level and systematic uncertainty in SK-III data analysis due to
 - Water system modification
 - Improvement of reconstruction tools
 - Precise calibration and upgrade of detector simulation
- Solar flux, energy spectrum and oscillation results are upgraded including SK-III data
- Measurement in SK-IV phase is on-going, after upgrading front-end electronics and DAQ system.

Definition of SK χ^2

Stat.+Energy-uncorrelated sys

Energy correlated sys.

Spectrum fit

$$\chi^2 = \sum_p^{N_{phase}} \left(\sum_i^{N_{bin,p}} \frac{(d_{i,p} - \rho_{i,p})^2}{\sigma_{i,p}^2} + \delta_{S,p}^2 + \delta_{R,p}^2 \right) + \delta_B^2 + \frac{(\beta - \beta_{NC})^2}{\sigma_{NC}^2} + \frac{(\eta - 1)^2}{\sigma_{hep}^2}$$

$$+ \sum_p^{N_{phase}} \Delta \chi_{t.v.,p}^2(\beta, \eta, \delta_B, \delta_{S,p}, \delta_{R,p})$$

Time variation

β rate is constrained by SNO NC flux

hep rate is constrained by SSM flux and uncertainty.

oscillated/unoscillated of ${}^8\text{B}$ (hep) flux

$$d_i = \frac{\text{Data}_i}{{}^8\text{B}_i^{\text{SSM}} + hep_i^{\text{SSM}}}, \quad \rho_i = \frac{\beta b_i + \eta h_i}{f_i}$$

$$b_i = \frac{{}^8\text{B}_i^{\text{osc}}(\Delta m^2, \tan^2 \theta)}{{}^8\text{B}_i^{\text{SSM}} + hep_i^{\text{SSM}}}, \quad h_i = \frac{hep_i^{\text{osc}}(\Delta m^2, \tan^2 \theta)}{{}^8\text{B}_i^{\text{SSM}} + hep_i^{\text{SSM}}}$$

correlation function

${}^8\text{B}$ spectrum shape

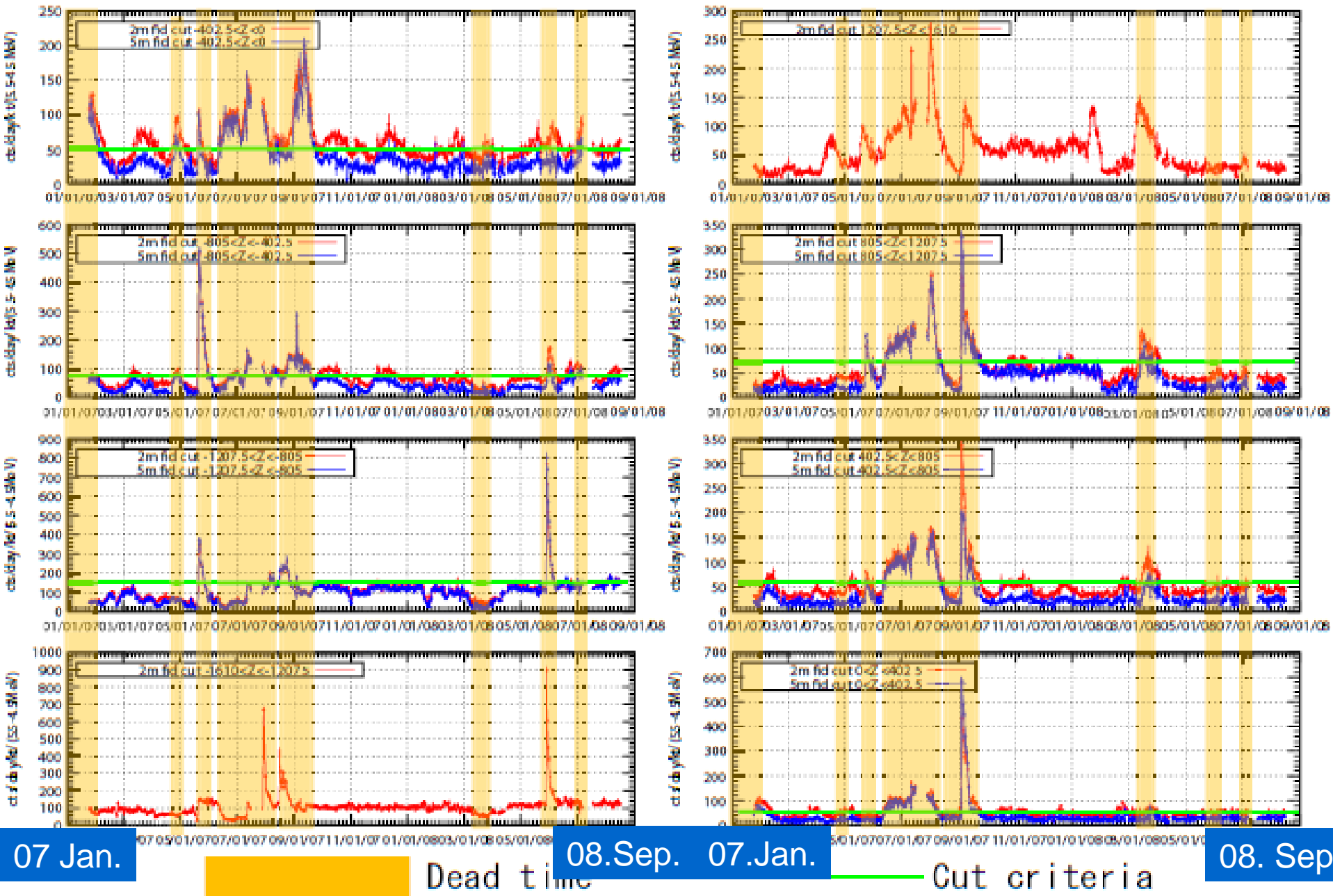
energy scale

energy resolution

$$f_i(\delta_B, \delta_S, \delta_R) = f_i^B(\delta_B) \times f_i^S(\delta_S) \times f_i^R(\delta_R)$$

β , η and δ s are chosen to minimize the spectrum fit χ^2 .

Select period with stable event rate



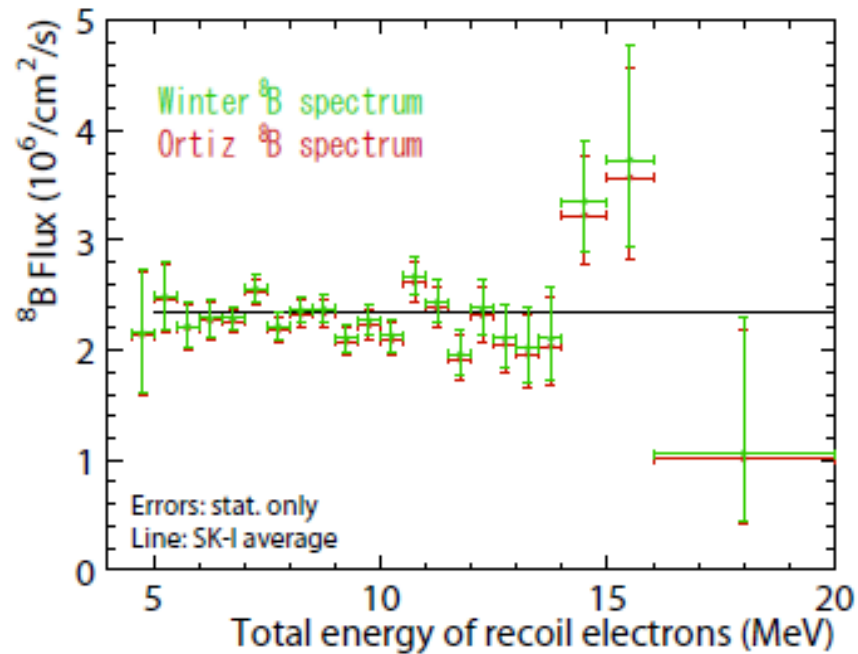


Figure 12.3: SK-III data /SSM (BP2004) with Winter and Ortiz ${}^8\text{B}$ spectrum. Green shows SSM with Winter ${}^8\text{B}$ spectrum, and red shows SSM with Ortiz ${}^8\text{B}$ spectrum.

^8B flux comparison

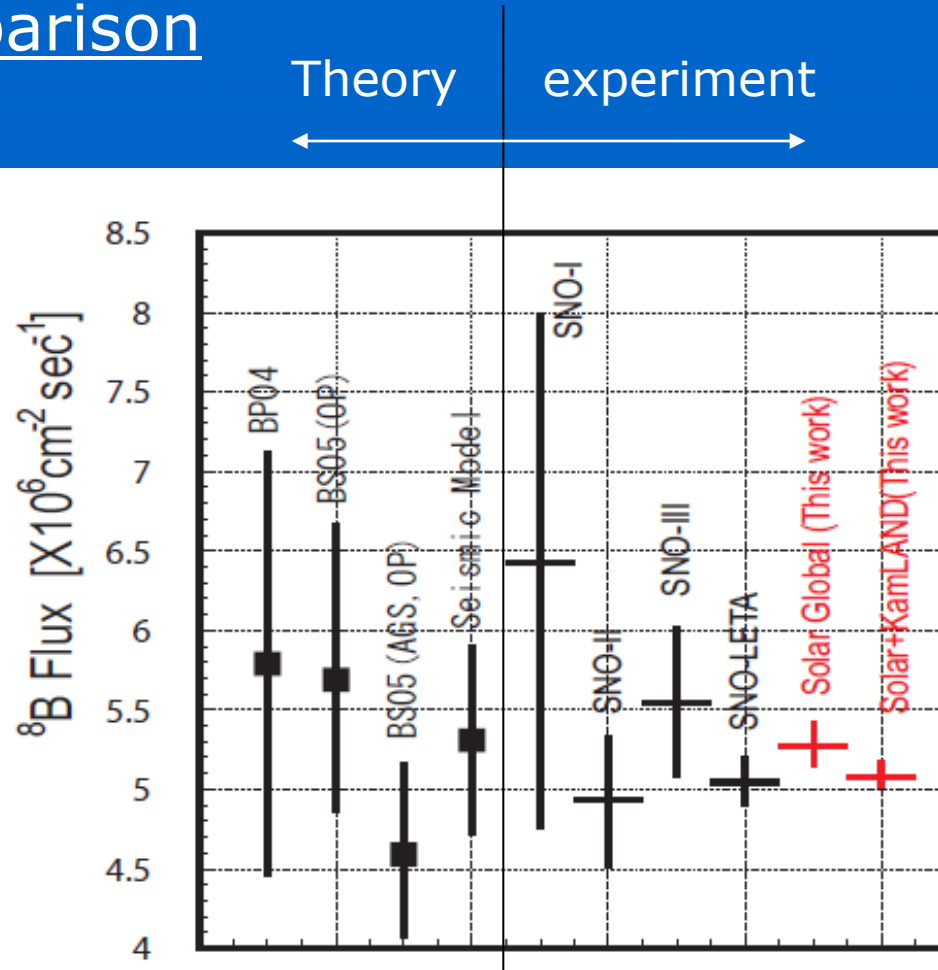
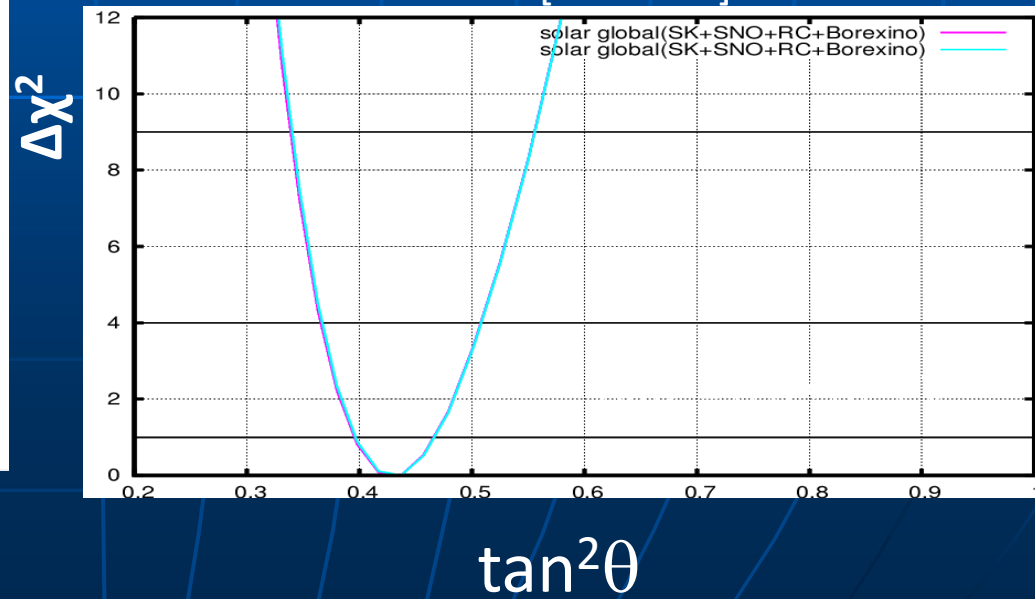
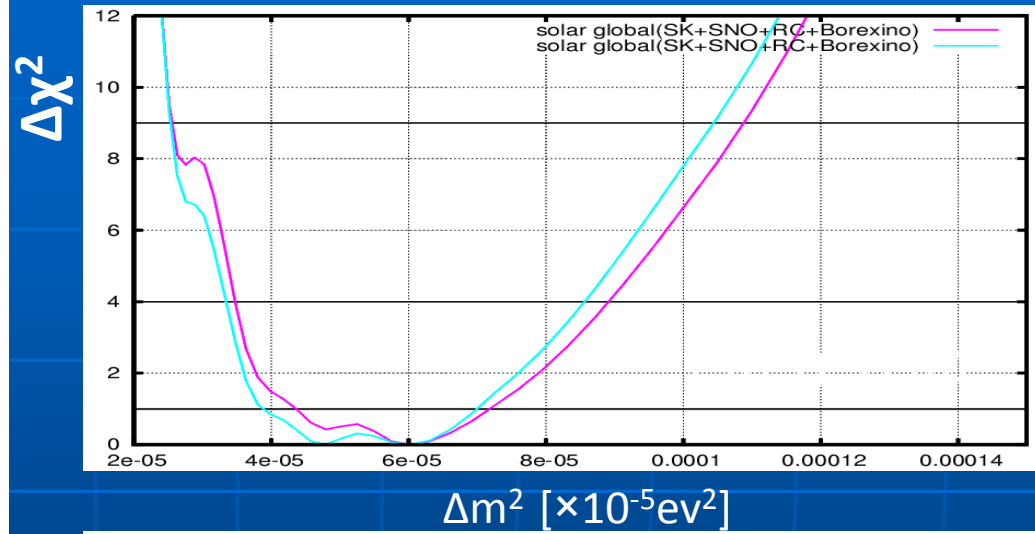
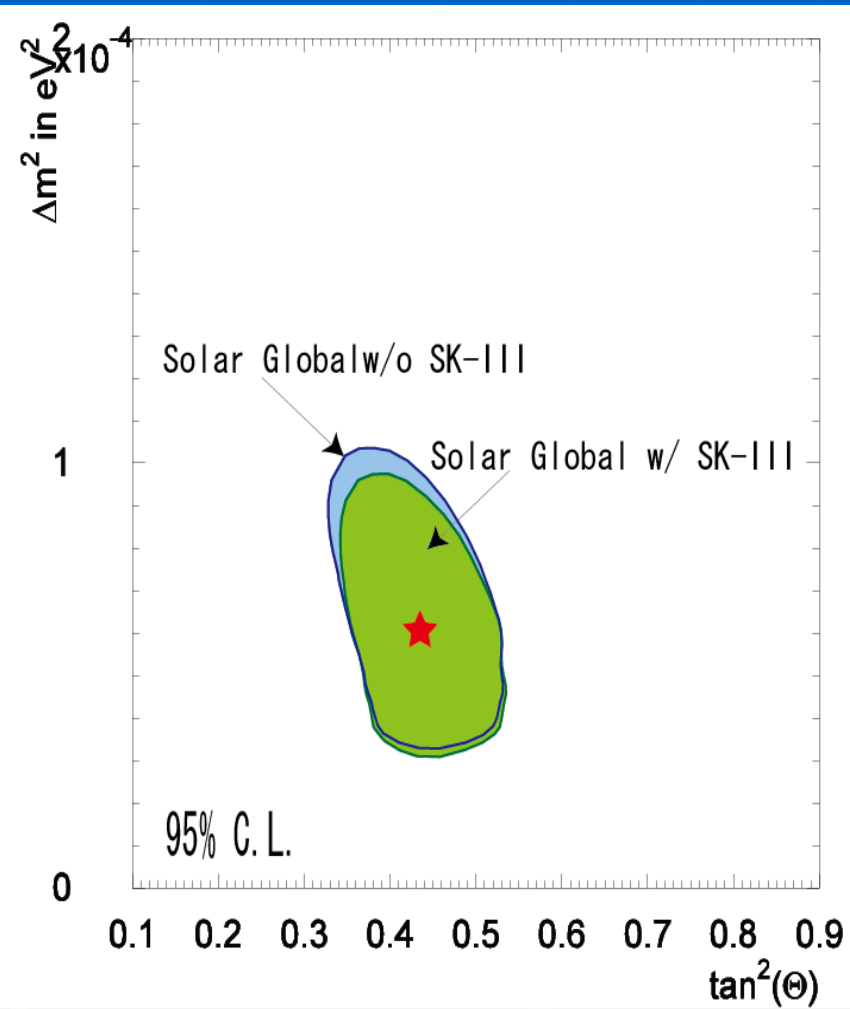


Figure 12.6: Comparison of the ^8B flux between SNO results and the results obtained by this thesis. the error size corresponds to 1σ uncertainty of (stat.+sys.). Square mark shows theoretical predictions and cross marks shows experimental results.

Contribution of SK-III result



Definition of χ^2 s for global analysis

SK spectrum+SNO flux fit

$$\chi_{SK+SNO}^2 = \sum_p^{N_{phase}} \left(\sum_i^{N_{bin,p}} \frac{(d_{i,p} - \rho_{i,p})^2}{\sigma_{i,p}^2} + \delta_{S,p}^2 + \delta_{R,p}^2 \right) + \delta_B^2 + \frac{(\eta - 1)^2}{\sigma_{hep}^2} + \chi_{SNO, flux}^2(\beta, \eta)$$

$$+ \sum_p^{N_{phase}} \Delta \chi_{t.v.,p}^2(\beta, \eta, \delta_B, \delta_{S,p}, \delta_{R,p}) + \sum_{p=1}^2 \frac{(ADN_{CC}^p - ADN_{prde}^p(\beta, \eta))^2}{(\sigma_{ADN}^p)^2}$$

SK Time variation
SNO CC flux Day/Night asymmetry

$$\chi_{SNO, flux}^2(\beta, \eta) = \sum_{p=1}^3 \frac{(D_{CC}^p - (\beta B_{CC}^p + \eta H_{CC}^p))^2}{(\sigma_{cc}^p)^2} + \frac{(D_{NC} - (\beta B_{SSM} + \eta H_{SSM}))^2}{(\sigma_{NC})^2}$$

β , η and δ s are chosen to minimize (SK spectrum+SNO flux fit) χ^2 .

$$\chi_{GaCl}^2 = \sum_{n,m=1}^{N(=2)} (R_n^{\exp t} - R_n^{theor}) [\sigma_{nm}^2]^{-1} (R_m^{\exp t} - R_m^{theor})$$

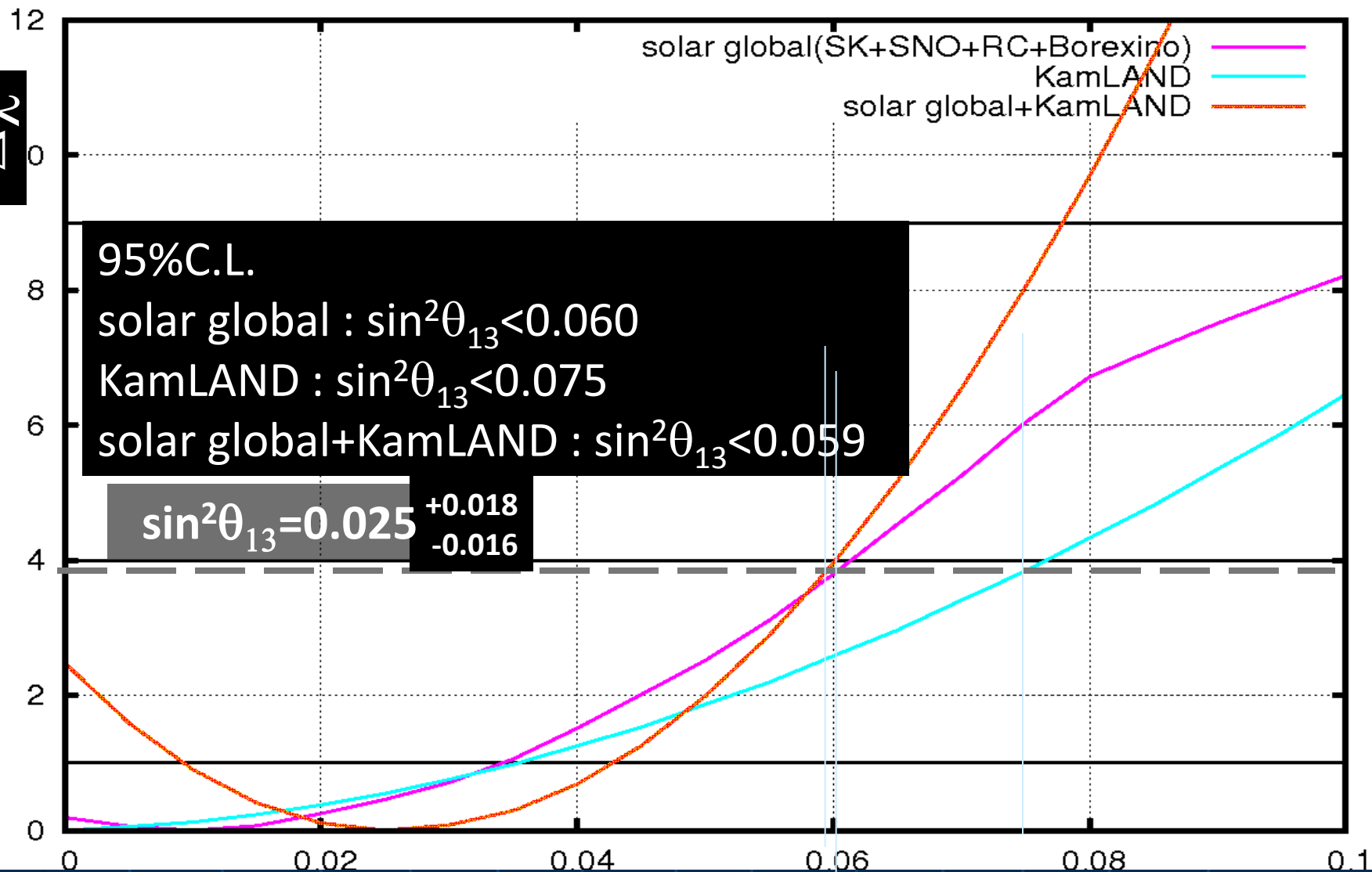
Ga/Cl

$$\chi_{GaClBore}^2 = \sum_{n,m=1}^{N(=3)} (R_n^{\exp t} - R_n^{theor}) [\sigma_{nm}^2]^{-1} (R_m^{\exp t} - R_m^{theor})$$

Ga/Cl/Borexino

1D plot – this time analysis

$\Delta\chi^2$



95% C.L.

solar global : $\sin^2\theta_{13} < 0.060$

KamLAND : $\sin^2\theta_{13} < 0.075$

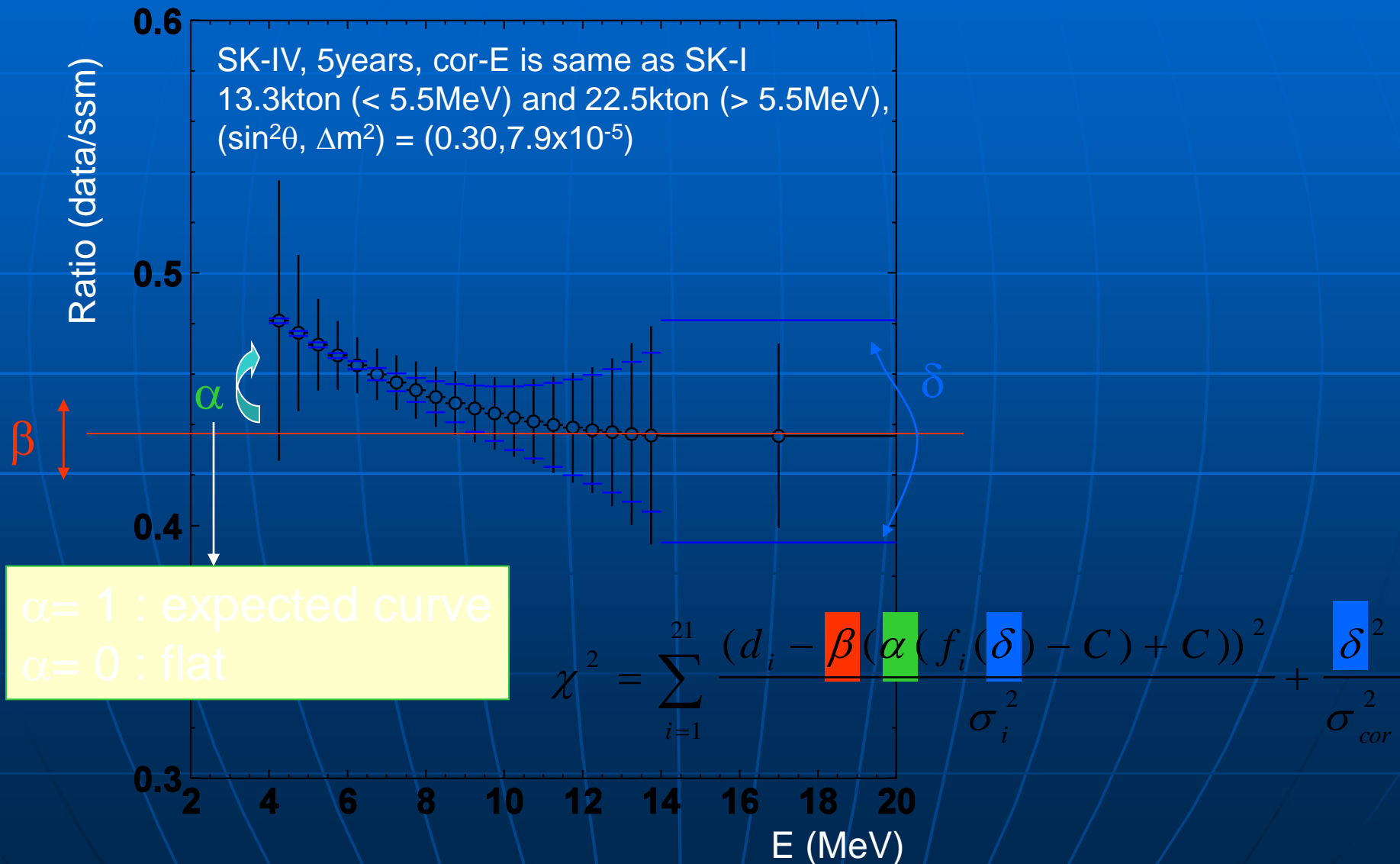
solar global+KamLAND : $\sin^2\theta_{13} < 0.059$

$\sin^2\theta_{13} = 0.025$ $+0.018$
 -0.016

preliminary $3\sigma_{-7.ps}$

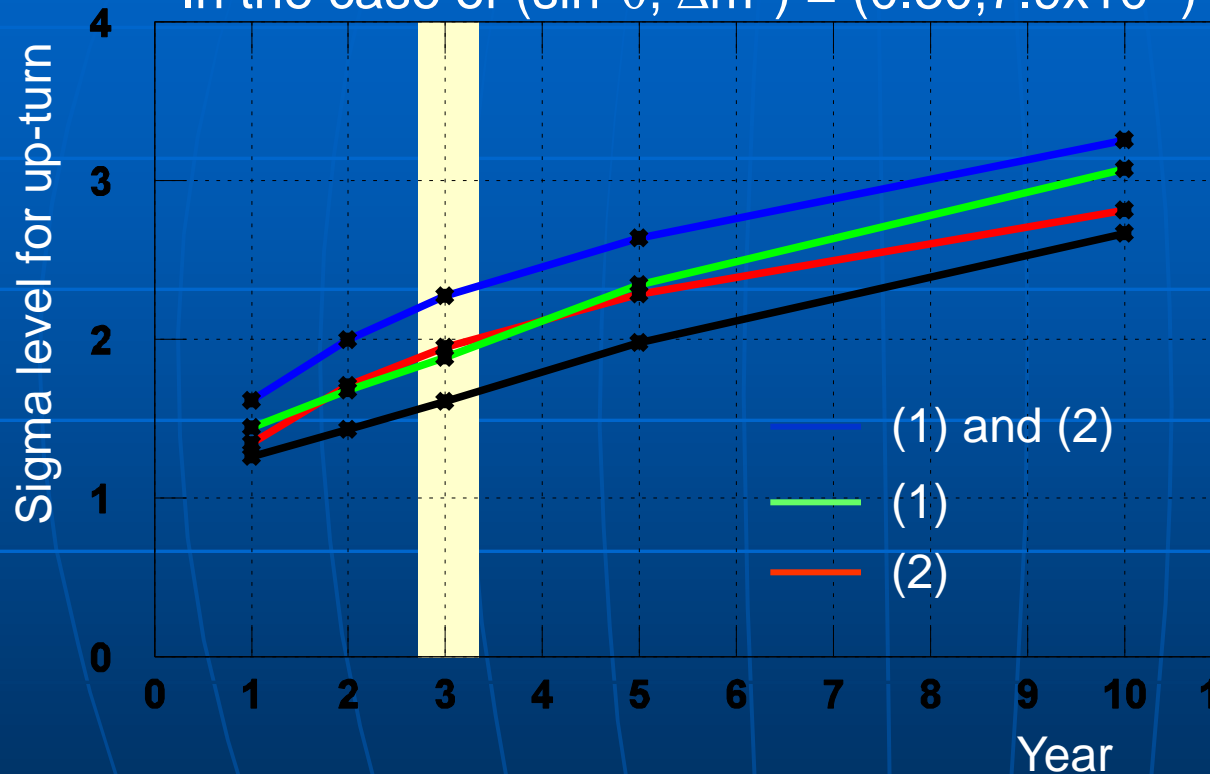
$\sin^2\theta_{13}$

Sensitivity calculation



Sensitivity of the upturn measurement

In the case of $(\sin^2\theta, \Delta m^2) = (0.30, 7.9 \times 10^{-5})$



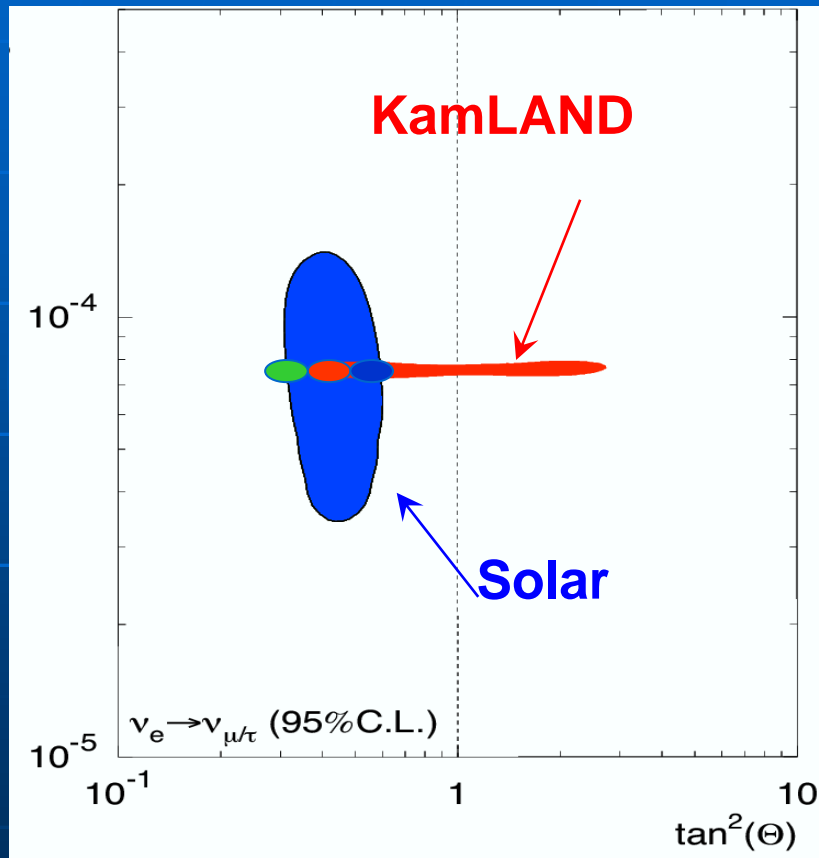
- First target : 2 sigma level up-tern discovery for 3 years observation. (or exclude the up-tern)
- Need to enlarge fiducial volume with low BG as large as possible
- Also the reduction of the energy correlated systematic error is important.

(1) Enlarge fiducial volume to 22.5kton with low B.G.

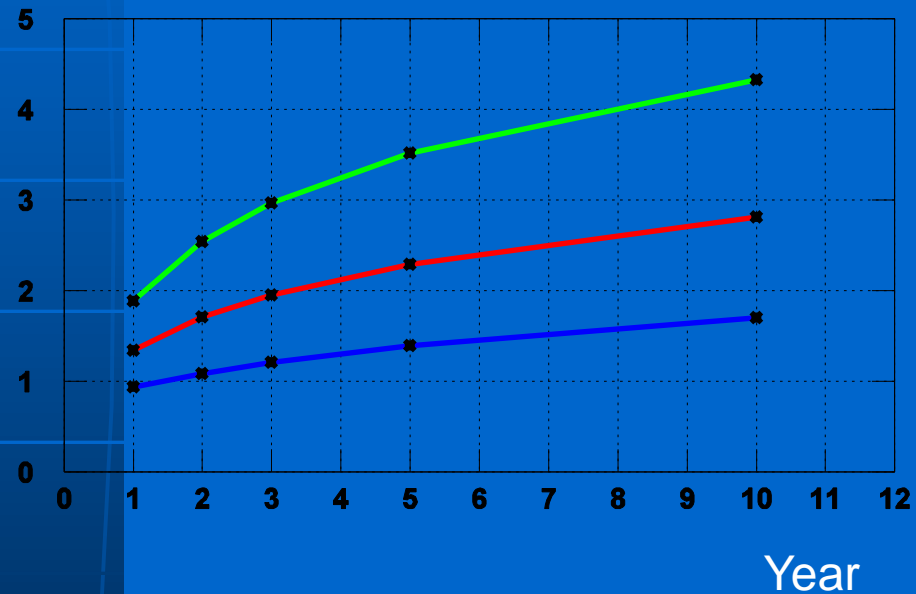
(2) Half energy correlated systematic error as SK-1.

The black line shows the 13.3kton ($<5.5\text{MeV}$), 22.5kton ($>5.5\text{MeV}$) fiducial volume with the same energy correlated error as SK-1

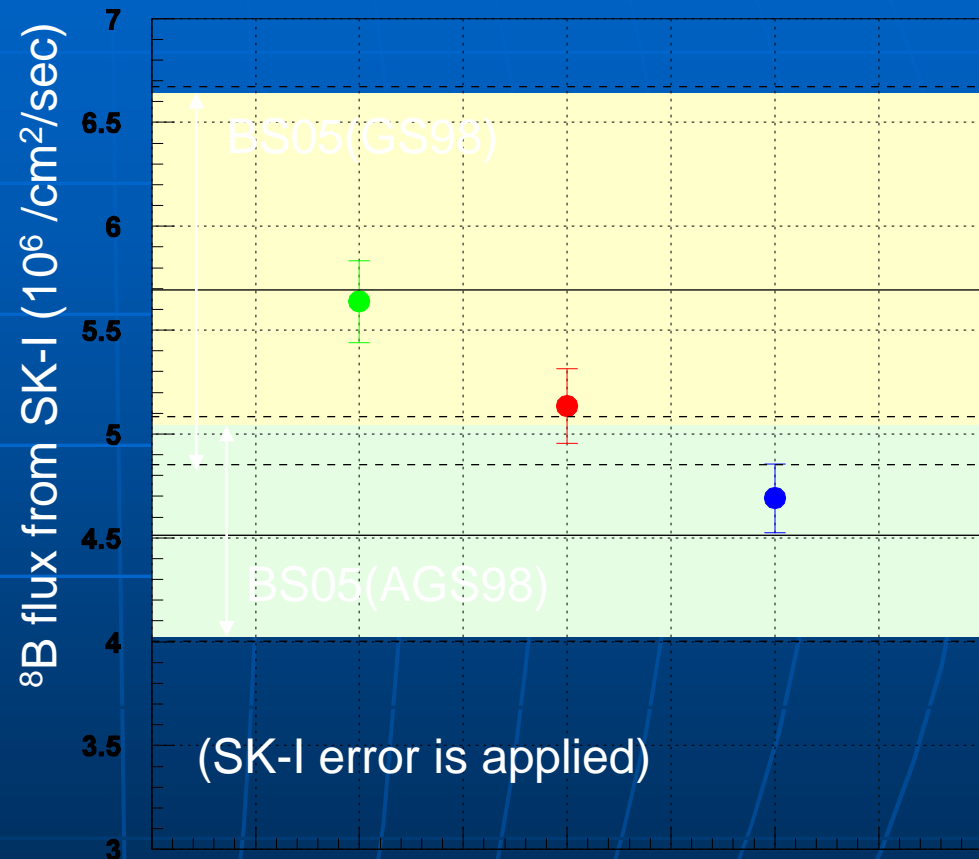
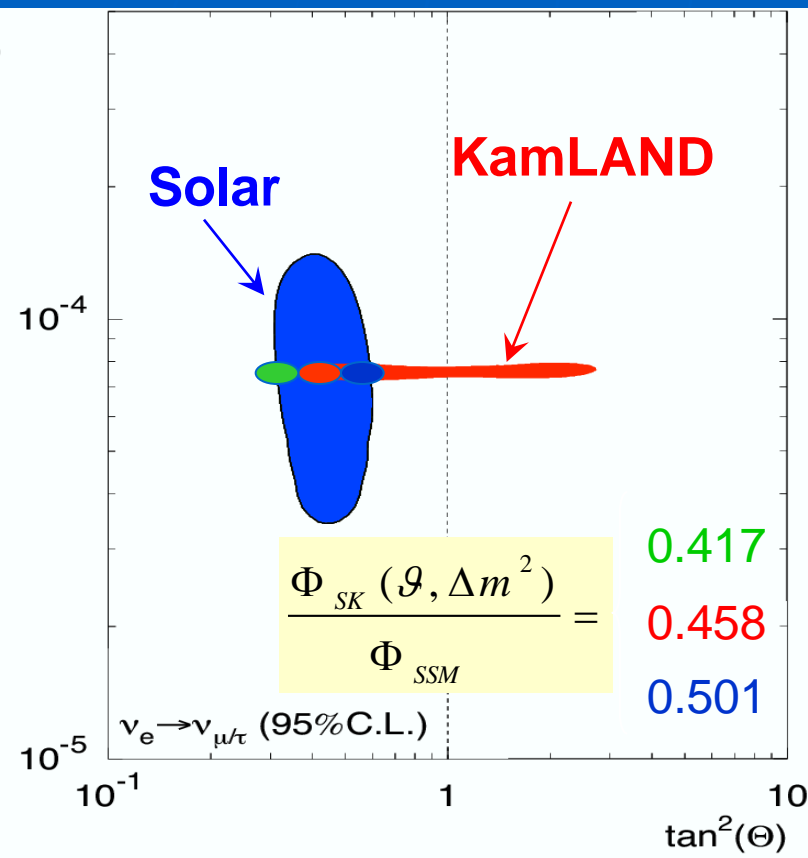
Oscillation parameter dependence



The correlated error is **half** as SK-1
 13.3kton (< 5.5MeV) and 22.5kton (> 5.5MeV)



Flux measurement in SK



If θ_{12} is determined, the precise ^8B flux measurement in SK may be possible to contribute the improvement of the Solar Model.